Phagocytosis

Cultured cells (2×10^5/mL) were incubated with FITC-dextran (40 000 molecular weight; Sigma Chemical) or FITC-latex beads (2 μm; Polysciences, Warrington, PA) for 1 hour at 37°C or 4°C. The uptake of FITC-dextran and FITC-latex beads was halted by the addition of cold 1% FBS PBS. After washing 3 times with 1% FBS PBS, cells were analyzed on a FACS flow cytometer.[28,29]

Results

$CD15^+CD14^-$ neutrophils generate macrophages

We isolated $CD15^+CD14^-$ cells from human blood samples. Portions of May-Grünwald-Giemsa–, MPO-, and double-specific/nonspecific esterase–stained preparations are presented in Figure 1A. The $CD15^+CD14^-$ cell fraction consisted of myelocytes, metamyelocytes, band cells, and segmented cells. Proportions of myelocytes, metamyelocytes, band cells, and segmented cells were 0.6% ± 0.2%, 9.2% ± 2.5%, 87.6% ± 2.5%, and 2.6% ± 0.4%, respectively (n = 5). $CD15^+CD14^-$ cells were positive for MPO and specific esterase but negative for nonspecific esterase. These staining patterns were found in all portions of cytospin preparations. We analyzed the cell cycle characteristics of $CD15^+CD14^-$ cells. All $CD15^+CD14^-$ cells were found in G_1 phase of the cell cycle (Figure 1B), supporting the notion that these cells are postmitotic. The expression of MPO, M-CSFR, lactoferrin, mannose receptor, and HLA-DR was assessed by phenotypic analysis (Figure 1C). $CD15^+CD14^-$ cells were MPO^+, M-$CSFR^-$, $lactoferrin^+$, $mannose\ receptor^-$, and $HLA\text{-}DR^-$, a finding compatible with typical features of mature neutrophils. $CD14^+$ cells were also prepared from blood samples. Cultures of $CD14^+$ cells in the presence of M-CSF gave rise to cells with small nuclei and intracytoplasmic vacuoles. These

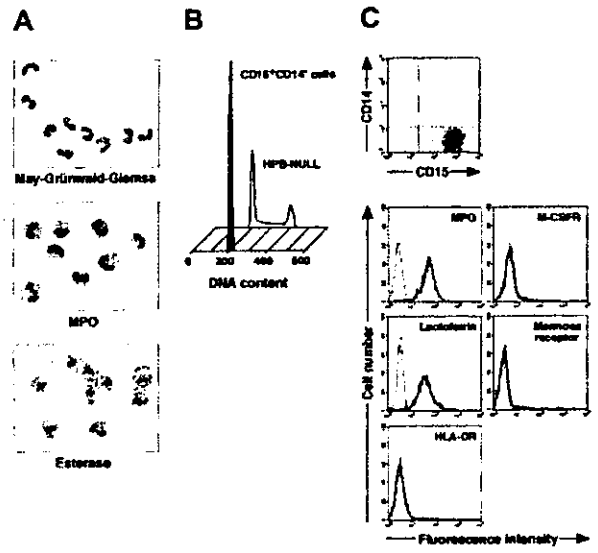

Figure 1. Cytochemistry and phenotype of freshly isolated $CD15^+CD14^-$ cells. (A) Photographs of May-Grünwald-Giemsa–, MPO-, and double-specific/nonspecific esterase–stained cytospin preparations; original magnification, × 400. (B) Nuclear DNA analysis of $CD15^+CD14^-$ cells was performed using a FACSCalibur flow cytometer. HPB-NULL cells were used as controls. Cell cycle distribution of HPB-NULL cells was as follows: with G_1 phase, 42.9%; S phase, 30.5%; and G_2/M phase, 26.6%. (C) The expression of CD15/CD14, MPO, M-CSFR, lactoferrin, mannose receptor, and HLA-DR was analyzed using a FACSCalibur flow cytometer. In the histograms, the thick and thin lines show the expression of the indicated molecules and isotype controls, respectively. Representative data from 5 independent experiments are shown.

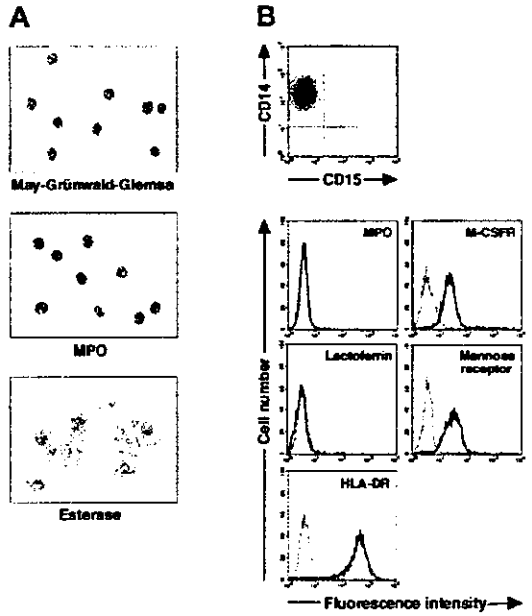

Figure 2. Cytochemistry and phenotype of cells obtained from 7-day culture of freshly isolated $CD14^+$ cells with M-CSF. (A) Photographs of May-Grünwald-Giemsa–, MPO-, and double specific/nonspecific esterase–stained cytospin preparations; original magnification, × 400. (B) The expression of CD15/CD14, MPO, M-CSFR, lactoferrin, mannose receptor, and HLA-DR was analyzed using a FACSCalibur flow cytometer. In the histograms, the thick and thin lines show the expression of the indicated molecules and isotype controls, respectively. Yield of cultured cells was 52.8% ± 9.8% (n = 5). Representative data from 5 independent experiments are shown.

cells showed nonspecific esterase activity but not MPO or specific esterase activity (Figure 2A), and they exhibited the phenotype of $CD15^-$ $CD14^+$, MPO^-, M-$CSFR^+$, $lactoferrin^-$, $mannose\ receptor^+$, and $HLA\text{-}DR^+$ (Figure 2B), which suggested that the resultant cells were macrophages. $CD15^+CD14^-$ cells were also cultured in the presence of M-CSF for 7 days. The yield was less than 2% of the starting population. Surviving cells retained the features of neutrophils (data not shown).

To determine whether postmitotic neutrophils have the potential to alter the lineage, we attempted to drive $CD15^+CD14^-$ cells to become cells of a monocyte/macrophage lineage, using cultures supplemented with cytokines. The combination of GM-CSF, M-CSF, TNF-α, and IFN-γ was chosen because GM-CSF, M-CSF, TNF-α, and IFN-γ are known to favor the differentiation of monocytes and their progenitors into macrophages.[1,30-36] Because M-CSF is a cytokine specific for, and late-acting in, a monocyte/macrophage lineage, we cultured $CD15^+CD14^-$ cells in the presence of GM-CSF, TNF-α, and IFN-γ for 11 days and subsequently replated the cells in cultures with M-CSF alone. On day 18 after the initiation of culture, cultured cells were harvested and characterized in morphologic, cytochemical, and phenotypic analyses. These cells had macrophage morphology (Figure 3A). Their MPO or specific esterase activity was not detected using light microscopy; however, the nonspecific esterase reaction was positive. CD14 expression was induced in a substantial, although not the entire, population of the resultant cells, but CD15 expression was completely lost (Figure 3B). When compared with freshly isolated $CD15^+CD14^-$ cells, the resultant cells did not entirely down-regulate MPO and lactoferrin yet they considerably up-regulated M-CSFR, mannose receptor, and HLA-DR. This culture condition yielded 1.8% ± 0.6% (n = 5) of the starting $CD15^+CD14^-$ cell population. These data suggest that GM-CSF, TNF-α, IFN-γ, and M-CSF allow $CD15^+CD14^-$ cells to become macrophages.

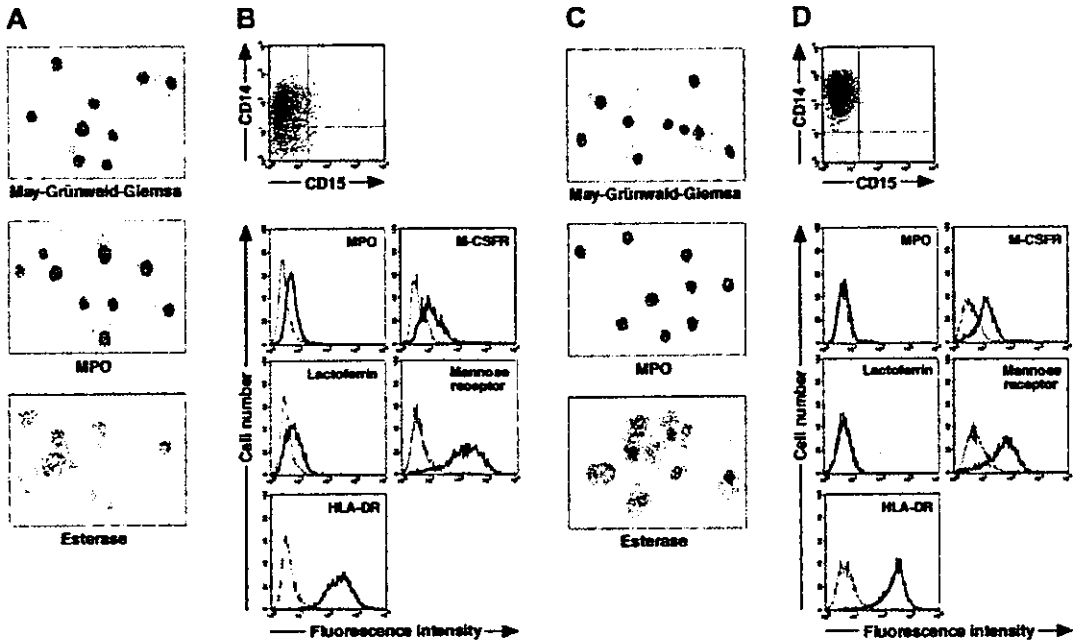

Figure 3. Cytochemistry and phenotype of cells obtained from culture of freshly isolated CD15⁺CD14⁻ neutrophils. (A-B) Freshly isolated CD15⁺CD14⁻ neutrophils were cultured with GM-CSF, TNF-α, and IFN-γ for 11 days, followed by additional 7-day culture with M-CSF alone. (C-D) Freshly isolated CD15⁺CD14⁻ neutrophils were cultured with GM-CSF, TNF-α, IFN-γ, and IL-4 for 11 days, followed by additional 7-day culture with M-CSF alone. (A,C) Photographs of May-Grünwald-Giemsa-, MPO-, and double specific/nonspecific esterase–stained cytospin preparations; original magnification, × 400. (B,D) The expression of CD15/CD14, MPO, M-CSFR, lactoferrin, mannose receptor, and HLA-DR was analyzed using a FACSCalibur flow cytometer. In the histograms, the thick and thin lines show the expression of the indicated molecules and isotype controls, respectively. Representative data from 5 independent experiments are shown.

Next, we searched for cytokine(s). The addition of cytokines to cultures would allow cells derived from CD15⁺CD14⁻ cells to acquire features more typical of macrophages. After testing several cytokines, we found that the appropriate conditions could be satisfied by supplementation with IL-4. When cultured with GM-CSF, TNF-α, IFN-γ, and IL-4 for 11 days and with M-CSF alone for 7 days, CD15⁺CD14⁻ cells gave rise to cells with morphologic characteristics of macrophages. The resultant cells were negative for MPO and specific esterase activities and positive for nonspecific esterase activity on cytospin preparations (Figure 3C). Phenotypic analysis showed that the resultant cells lacked CD15 and exclusively expressed CD14. MPO and lactoferrin were completely down-regulated, whereas the high levels of M-CSFR, mannose receptor, and HLA-DR expression were retained (Figure 3D), as in the macrophage phenotype induced from CD14⁺ cells by M-CSF. Strikingly, the yield increased to 15.1% ± 3.6% (n = 5) of the starting CD15⁺CD14⁻ cell population. These observations unambiguously demonstrated a cytokine-induced lineage switch of postmitotic neutrophils to macrophages. We also cultured CD15⁺CD14⁻ cells in the presence of GM-CSF, TNF-α, IFN-γ, and IL-4 for 11 days and analyzed their phenotypes using flow cytometry. Cultured cells expressed neither CD15 nor CD14 (Figure 4A). MPO and lactoferrin were detected at low levels, whereas the expression levels of M-CSFR, mannose receptor, and HLA-DR were high (Figure 4B). These data suggest that the expression levels of molecules that characterize postmitotic neutrophils or macrophages are not simultaneously altered during this lineage switch program.

Gene expression profiles of CD15⁺CD14⁻ neutrophils and macrophages

Given that the combination of cytokines consisting of GM-CSF, TNF-α, IFN-γ, IL-4, and M-CSF allowed for the generation of macrophages from CD15⁺CD14⁻ neutrophils, as determined by morphologic, cytochemical, and phenotypic analyses, we compared the gene expression profiles of freshly isolated CD15⁺CD14⁻ neutrophils, CD15⁺CD14⁻ neutrophil–derived macrophages, and CD14⁺ cell–derived macrophages using high-density oligonucleotide microarrays. Because every microarray was repeated twice, the mean expression intensity was calculated for each gene and was used for the following analysis. Among our expression data set, first searched were the genes expressed abundantly in CD15⁺CD14⁻ neutrophils but not in CD14⁺ cell–derived macrophages. Table 1 shows 10 such genes that had an expression level of more than 100 arbitrary units in CD15⁺CD14⁻ neutrophils and the highest ratio of the expression level between CD15⁺CD14⁻ neutrophils and CD14⁺

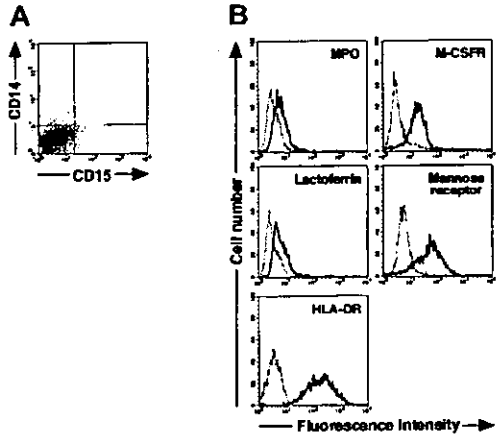

Figure 4. Cytochemistry and phenotype of cells obtained from culture of freshly isolated CD15⁺CD14⁻ neutrophils with GM-CSF, TNF-α, IFN-γ, and IL-4 for 11 days. (A) Expression pattern of CD15/CD14. (B) The expression of CD15/CD14, MPO, lactoferrin, M-CSFR, mannose receptor, and HLA-DR was analyzed using a FACSCalibur flow cytometer. In the histograms, the thick and thin lines show the expression of the indicated molecules and isotype controls, respectively. Representative data from 5 independent experiments are shown.

Table 1. Genes specifically expressed in CD15$^+$CD14$^-$ neutrophils

Gene symbol	GenBank accession no.	CD15$^+$CD14$^-$ neutrophil/ CD14$^+$ cell-derived macrophage ratio	CD15$^+$CD14$^-$ neutrophils	CD14$^+$ cell-derived macrophages	CD15$^+$CD14$^-$ neutrophil-derived macrophages
bA209J19.1	AL390736	5412.83	1623.85	0.30	0.60
LTF	NM_002343	2795.52	3773.95	1.35	1.50
DEFA3	NM_004084	1142.16	15 761.80	13.80	9.65
S100P	NM_005980	1099.67	3189.05	2.90	28.05
SGP28	NM_006061	699.78	314.90	0.45	0.45
CEACAM8	M33326	588.24	1323.55	2.25	3.30
LCN2	NM_005564	550.64	2945.90	5.35	8.90
DEFA4	NM_001925	499.83	2849.05	5.70	3.85
CD24	BG327863	474.81	759.70	1.60	8.75
FIZZ3	NM_020415	452.96	1223.00	2.70	5.90

Mean expression levels of genes in CD15$^+$CD14$^-$ neutrophils, CD14$^+$ cell–derived macrophages, and CD15$^+$CD14$^-$ neutrophil–derived macrophages are shown in arbitrary units. The ratio between the first 2 is indicated in the CD15$^+$CD14$^-$ neutrophil/CD14$^+$ cell–derived macrophage ratio.

cell–derived macrophages. Interestingly, all these CD15$^+$CD14$^-$ neutrophil-specific genes were also transcriptionally silent in CD15$^+$CD14$^-$ neutrophil–derived macrophages, as in CD14$^+$ cell–derived macrophages. A well-known marker for granulocytes, CD24 (GenBank accession number AA761181) was only expressed in CD15$^+$CD14$^-$ neutrophils but not in CD15$^+$CD14$^-$ neutrophil–derived macrophages or CD14$^+$ cell–derived macrophages. Conversely, we also tried to extract CD14$^+$ cell–derived, macrophage-specific genes by comparing CD14$^+$ cell–derived macrophages and CD15$^+$CD14$^-$ neutrophils (Table 2). Again, expression levels of these genes in the CD15$^+$CD14$^-$ neutrophil–derived macrophages were highly similar to those in CD14$^+$ cell–derived macrophages. A monocyte/macrophage-specific cell surface antigen, CD163 (Z22969), was abundantly expressed in the CD15$^+$CD14$^-$ neutrophil–derived macrophages and the CD14$^+$ cell–derived macrophages, but not in the CD15$^+$CD14$^-$ neutrophils. Hierarchical clustering analysis of these lineage-specific genes showed the similarity between gene expression profiles of CD15$^+$CD14$^-$ neutrophil–derived macrophages and CD14$^+$ cell–derived macrophages (Figure 5A). Next, to statistically examine this similarity, we directly compared the 4 expression data sets of CD15$^+$CD14$^-$ neutrophils (n = 2) and CD14$^+$ cell–derived macrophages (n = 2) and attempted to identify the genes, whose expression was different in the 2 groups (Welch ANOVA, $P < .001$). The expression profiles of such 9 lineage-dependent genes (Table 3) were then used to measure the similarity between CD14$^+$ cell–derived macrophages and the other 2 groups. As shown in Figure 5B, 2-way clustering analysis[37] of 6 data sets (3 groups) clearly indicated that, with regard to gene expression profile, CD15$^+$CD14$^-$ neutrophil–derived macrophages were similar to CD14$^+$ cell–derived macrophages, separated from CD15$^+$ CD14$^-$ neutrophils.

Phagocytic activity of CD15$^+$CD14$^-$ neutrophil–derived macrophages

Morphology, cytochemistry, phenotype, and gene expression of cultured cells in the presence of GM-CSF, TNF-α, IFN-γ, IL-4, and M-CSF indicated that CD15$^+$CD14$^-$ neutrophils became macrophages. Therefore, we next evaluated the phagocytic activity of these macrophages using FITC-dextran and FITC-latex beads. The potential for CD15$^+$CD14$^-$ neutrophil–derived macrophages to incorporate dextran and latex beads was comparable to that of CD14$^+$ cell–derived macrophages (Figure 6).

Proliferative characteristics during culture

It is possible that macrophages induced from CD15$^+$CD14$^-$ neutrophils were derived from a small number of hematopoietic progenitor cells for macrophages that contaminated the CD15$^+$CD14$^-$ cell population and consequently proliferated. To exclude this possibility, we analyzed proliferative characteristics of the cultured cells; representative data are presented in Figure 7. In Figure 7A, the yield of cultured cells was 15.1%, on day 18 of culture. Reactivity with Ki-67 and incorporation of BrdU were tested on the indicated days of culture.[24,38] Ki-67$^+$ or BrdU$^+$ cells were not evident throughout the culture. Ki-67 expression and BrdU incorporation were observed most and approximately 30%, respectively, of HPB-NULL cells, which served as positive controls. We also used the carboxyfluorescein diacetate succinimidyl ester

Table 2. Genes specifically expressed in CD14$^+$ cell-derived macrophages

Gene symbol	GenBank accession no.	CD14$^+$ cell-derived macrophage/CD15$^+$CD14$^-$ neutrophil ratio	CD14$^+$ cell-derived macrophages	CD15$^+$CD14$^-$ neutrophils	CD15$^+$CD14$^-$ neutrophil-derived macrophages
SEPP1	NM_005410	643.60	1769.90	2.75	1373.45
DAB2	NM_001343	307.52	1183.95	3.85	513.20
CD163	Z22969	256.43	2602.75	10.15	1034.35
ME1	NM_002395	197.02	551.65	2.80	310.10
CCL2	S69738	196.38	1708.50	8.70	351.10
ATP1B1	BC000006	180.35	775.50	4.30	408.85
FN1	BC005858	169.67	972.70	5.75	155.60
FN1	AK026737	162.44	1210.15	7.45	191.65
TGFBI	NM_000358	131.99	4045.55	30.65	3030.45
PMP22	L03203	129.14	1091.25	8.45	59.20

Mean expression levels of the genes in CD14$^+$ cell–derived macrophages, CD15$^+$CD14$^-$ neutrophils, and CD15$^+$CD14$^-$ neutrophil–derived macrophages are shown in arbitrary units. The ratio between the first 2 is indicated in the CD14$^+$ cell–derived macrophage/CD15$^+$CD14$^-$ neutrophil ratio.

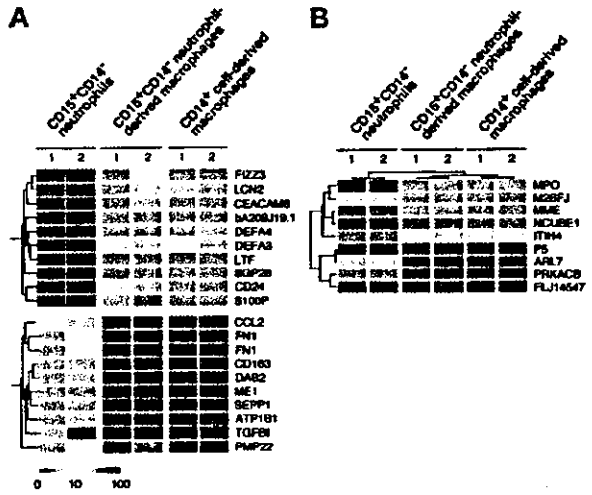

Figure 5. Expression profiles of neutrophil- and macrophage-specific genes. (A) Hierarchical clustering based on the expression intensities in $CD15^+CD14^-$ neutrophils, $CD15^+CD14^-$ neutrophil–derived macrophages, and $CD14^+$ cell–derived macrophages was conducted for 10 genes with a specific expression in $CD15^+CD14^-$ neutrophils and $CD14^+$ cell–derived macrophages (top panel) or in $CD14^+$ cell–derived macrophages (bottom panel). Each row represents a single gene on the microarray, and each column represents a separate sample. Expression intensity of each gene is shown color coded, according to the scale at the bottom, and the gene symbols are indicated on the right. Expression data of these genes are available on request. (B) The gene tree was constructed using 2-way clustering analysis of the genes that are differentially (Welch ANOVA, $P < .001$) expressed between $CD15^+CD14^-$ neutrophils and $CD14^+$ cell–derived macrophages. Each row represents a single gene on the microarray, and each column represents a separate sample. Expression intensity of each gene is shown color coded, according to the scale in panel A.

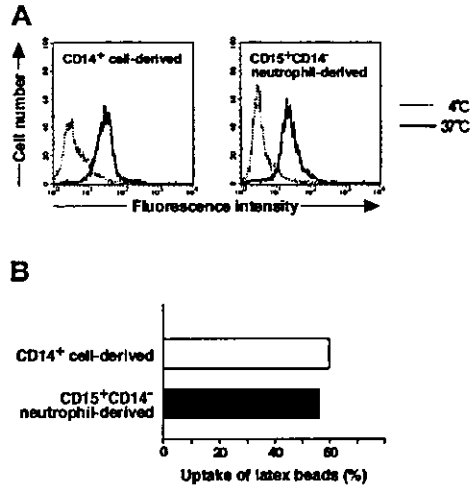

Figure 6. Phagocytic assay of $CD15^+CD14^-$ neutrophil–derived macrophages with FITC-dextran and FITC-latex beads. (A) $CD15^+CD14^-$ neutrophil– and $CD14^+$ cell–derived macrophages were incubated with FITC-dextran for 1 hour at 37°C or 4°C, washed with cold PBS supplemented with 1% FBS, and analyzed using a FACSCalibur flow cytometer. Data are presented using histograms. (B) $CD15^+CD14^-$ neutrophil– and $CD14^+$ cell–derived macrophages were incubated with FITC-latex beads for 1 hour at 37°C or 4°C, washed with cold PBS supplemented with 1% FBS, and analyzed with a FACSCalibur flow cytometer. Data are expressed as percentage of positive cells. Experiments were repeated 5 times with identical results.

(CFSE) labeling technique to confirm that $CD15^+CD14^-$ neutrophils passed through no cell division during culture.[25] Analysis of the CFSE labeling pattern in $CD8^+$ T cells, which had elicited several rounds of the cell cycle in response to CD3/CD28 T-cell expander beads, displayed a number of peaks of fluorescence (Figure 7B). However, the CFSE fluorescence remained a single peak in the cells generated by culturing $CD15^+CD14^-$ neutrophils with GM-CSF, TNF-α, IFN-γ, and IL-4 and subsequently with M-CSF alone. These data indicate that the generation of macrophages from the $CD15^+CD14^-$ cell population in culture is not associated with cell division.

Discussion

Lineage switch of normal primary cells has been noted in murine lymphoid progenitor cells.[21,22] Montecino-Rodriguez et al[21] observed that a subpopulation of B-cell precursors in the bone marrow gave rise not only to B cells but also to macrophages in cultures supplemented with IL-3, IL-6, *c*-kit ligand, and GM-CSF. Lee et al[22] demonstrated that fetal thymocytes differentiate into

Table 3. Genes with statistically different expression between $CD15^+CD14^-$ neutrophils and $CD14^+$ cell-derived macrophages

Gene symbol	GenBank accession no.
MPO	J02694
H2BFJ	NM_003524
MME	NM_007287
NCUBE1	AF151039
ITIH4	D38535
P5	BC001312
ARL7	NM_005737
PRKACB	AA130247
FLJ14517	AV7113053

Gene symbols and GenBank accession numbers are shown for genes that exhibited significant differences in expression level between the 2 groups (Welch ANOVA, $P < .001$).

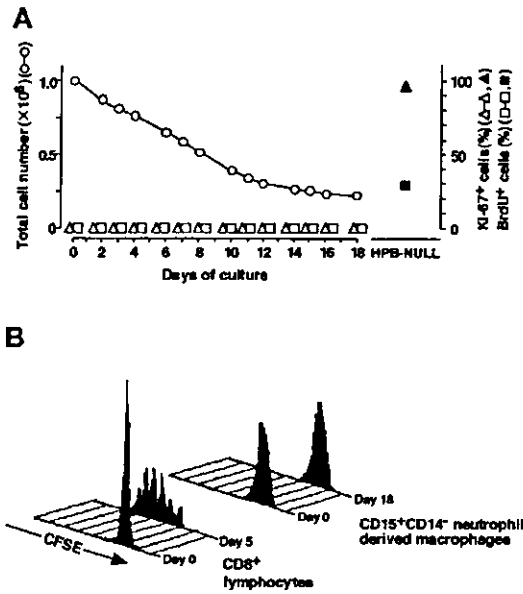

Figure 7. Analysis of proliferation profile. (A) $CD15^+CD14^-$ neutrophils were cultured with GM-CSF, TNF-α, IFN-γ, and IL-4 for 11 days, washed, and recultured with M-CSF alone for an additional 7 days. $CD15^+CD14^-$ neutrophils and the cultured cells were tested for Ki-67 staining and BrdU incorporation. Ki-67+ and $BrdU^+$ cells were counted using a FACSCalibur flow cytometer, and the numbers were expressed as percentages. HPB-NULL cells were used as positive controls. Numbers of cultured cells are also indicated. Representative data from 5 independent experiments are shown. (B) $CD15^+CD14^-$ neutrophils were cultured with GM-CSF, TNF-α, IFN-γ, and IL-4 for 11 days, washed, and recultured with M-CSF alone for another 7 days. $CD15^+CD14^-$ neutrophils and the cultured cells were incubated with CFSE. Cell division patterns were analyzed using a FACSCalibur flow cytometer. $CD8^+$ cells that underwent several rounds of the cell cycle in response to CD3/CD28 beads were used as positive controls. Experiments were repeated 5 times with identical results.

macrophages in the presence of M-CSF, IL-6, and IL-7 in vitro. A recent report stated that human B-cell progenitors obtained from cultures of cord blood $CD34^+CD10^-CD19^-$ cells gave rise to macrophages, NK cells, and T cells when exposed to the appropriate culture conditions.[23] Our study shows the lineage switch of human primary postnatal cells and further extends the existence of lineage switch to postmitotic cells. This notion is also supported by our observations in the microarray analysis that gene expression profiles of the resultant cells differed from those of the starting $CD15^+CD14^-$ neutrophils and were similar to those of $CD14^+$ cell–derived macrophages.

When we first cultured $CD15^+CD14^-$ neutrophils in the presence of GM-CSF, TNF-α, IFN-γ, and M-CSF, the resultant cells displayed morphologic and cytochemical features of macrophages. However, they preserved a low level of MPO activity and lactoferrin expression, as determined by flow cytometry. These data suggest that the resultant cells did not fully exhibit the phenotypic characteristics of macrophages. Our surprise was that the addition of IL-4 to cultures was sufficient for the resultant cells to acquire typical features of macrophages. It is also of note that in the presence of IL-4, the yield of the resultant cells increased to approximately 15%. The phagocytic activity of macrophages generated in IL-4–containing cultures was of a similar magnitude compared with that observed with $CD14^+$ cell–derived macrophages. Previous studies demonstrated the inhibitory activities of IL-4 on the development of monocytes/macrophages from progenitors supported by GM-CSF.[39,40] IL-4 has the potential to suppress TNF-α–induced effects on hematopoietic cells.[41] IL-4 also down-regulates the expression of 2 distinct receptors for TNF-α, p60, and p80 and induces shedding of these receptors, resulting in blockage of the cellular signaling elicited by TNF-α.[42] Moreover, several investigators have shown that IL-4 antagonizes IFN-γ–induced responses in human myeloid progenitor and mature cells.[43-45] Therefore, we have no plausible explanation for the mechanism of action of IL-4 on $CD15^+CD14^-$ neutrophils during their lineage switch to macrophages. Complex networks by multiple cytokines may be involved in the generation of macrophages from $CD15^+CD14^-$ neutrophils. Interestingly, phenotypic analysis indicated that when $CD15^+CD14^-$ neutrophils turn their lineage toward macrophages, they lose CD15 expression and acquire CD14. This finding demonstrates that the down-regulation of CD15 occurs before the up-regulation of CD14. The cascade of several different events may lead to the lineage conversion of $CD15^+CD14^-$ neutrophils to macrophages.

Our concern was whether a rare population of hematopoietic progenitors, contaminating the $CD15^+CD14^-$ fraction, could proliferate and differentiate into macrophages. If such were the case, the cultured cells would show signs of proliferation at several time points during culture. To address this issue, we used Ki-67 antibody staining, BrdU incorporation, and CFSE labeling. Neither $Ki\text{-}67^+$ nor $BrdU^+$ cells were detectable throughout culture, suggesting that cell division did not occur. In addition, if cultured cells had a history of successive cell divisions, we would have expected to observe separate peaks of CFSE fluorescence in the histogram. However, the narrow peak was observed with the resultant cells, as was the peak seen with the starting cell population. On the basis of these data and because the yield was approximately 15%, we assumed it was not possible for the cultured cells to have undergone more than one division throughout culture. Therefore, we propose that the generation of macrophages from $CD15^+CD14^-$ neutrophils with GM-CSF, TNF-α, IFN-γ, IL-4, and M-CSF was not caused by contamination of progenitor cells for macrophages but was the result of their lineage switch to macrophages. It was also possible that a small number of monocyte/macrophage precursors contaminated the starting $CD15^+CD14^-$ cell population. The yield in culture of $CD15^+CD14^-$ cells with M-CSF and neutrophilic features of a marginal number of the surviving cells could conceivably exclude this possibility.

Our observation that postmitotic neutrophils could generate macrophages raises the issue of developmental origin of human macrophages and may represent another developmental pathway from hematopoietic stem cells toward macrophages. However, it is unclear whether such a neutrophil-to-macrophage lineage switch occurs under physiologic conditions. Such a lineage switch may occur under specified conditions, such as inflammation, because GM-CSF, TNF-α, IFN-γ, IL-4, and M-CSF are inflammatory cytokines. Oehler et al[46] demonstrate that neutrophil granulocyte-committed cells acquire dendritic cell features in the presence of GM-CSF, IL-4, and TNF-α. Our results indicated that when $CD15^+CD14^-$ cells were cultured with GM-CSF, TNF-α, IFN-γ, and IL-4, the resultant cells exhibited a partial appearance of macrophages. IFN-γ may play a crucial role in the conversion of neutrophils into the macrophage lineage. In addition, it seems that neutrophils are capable of generating more types of mature cells than is generally recognized. Further studies on the reprogramming of already differentiated cells into other cell types are expected to yield new insights into events related to human hematopoiesis.

Acknowledgment

We thank M. Ohara (Fukuoka) for critical comments and language assistance.

References

1. Metcalf D. The molecular control of cell division, differentiation commitment and maturation in haemopoietic cells. Nature. 1989;339:27-30.
2. Ogawa M. Differentiation and proliferation of hematopoietic stem cells. Blood. 1993;81:2844-2853.
3. Boyd AW, Schrader JW. Derivation of macrophagelike lines from the pre-B lymphoma ABLS 8.1 using 5-azacytidine. Nature. 1982;297:691-693.
4. Klinken SP, Alexander WS, Adams JM. Hemopoietic lineage switch: v-*raf* oncogene converts Eμ-myc transgenic B cells into macrophages. Cell. 1988;53:857-867.
5. Borzillo GV, Ashmun RA, Sherr CJ. Macrophage lineage switching of murine early pre-B lymphoid cells expressing transduced *fms* genes. Mol Cell Biol. 1990;10:2703-2714.
6. Lindeman G., Adams JM, Cory S, Harris AW. B-lymphoid to granulocytic switch during hematopoiesis in a transgenic mouse strain. Immunity. 1994;1:517-527.
7. Nutt SL, Heavey B, Rolink AG, Busslinger M. Commitment to the B-lymphoid lineage depends on the transcription factor Pax5. Nature. 1999; 401:556-562.
8. Rolink AG, Nutt SL, Melchers F, Busslinger M. Long-term *in vivo* reconstitution of T-cell development by Pax5-deficient B-cell progenitors. Nature. 1999;401:603-606.
9. Kee BL, Murre C. Induction of early B cell factor (EBF) and multiple B lineage genes by the basic helix-loop-helix transcriptional factor E12. J Exp Med. 1998;188:699-713.
10. Kondo M, Scherer DC, Miyamoto T, et al. Cell-fate conversion of lymphoid-committed progenitors by instructive actions of cytokines. Nature. 2000;407:383-386.
11. Iwasaki-Arai J, Iwasaki M, Miyamoto T, Watanabe S, Akashi K. Enforced granulocyte/macrophage colony-stimulating factor signals do not support lymphopoiesis, but instruct lymphoid to myelomonocytic lineage conversion. J Exp Med. 2003;197:1311-1322.
12. Iwasaki J, Mizuno S-I, Wells RA, Cantor AB, Watanabe S, Akashi K. GATA-1 converts lymphoid and myelomonocytic progenitors into the megakaryocyte/erythrocyte lineages. Immunity. 2003;19:451-462.

13. Visvader JE, Elefanty AG, Strasser A, Adams JM. GATA-1 but not SCL induces megakaryocytic differentiation in an early myeloid line. EMBO J. 1992;11:4557-4564.
14. Kulessa H, Frampton J, Graf T. GATA-1 reprograms avian myelomonocytic cell lines into eosinophils, thromboblasts, and erythroblasts. Genes Dev. 1995;9:1250-1262.
15. Seshasayee D, Gaines P, Wojchowski DM. GATA-1 dominantly activates a program of erythroid gene expression in factor-dependent myeloid FDCW2 cells. Mol Cell Biol. 1998;18:3278-3288.
16. Yamaguchi Y, Zon LI, Ackeman SJ, Yamamoto M, Suda T. Forced GATA-1 expression in the murine myeloid cell line M1: induction of c-Mpl expression and megakaryocytic/erythroid differentiation. Blood. 1998;91:450-457.
17. Yamada T, Kihara-Negishi F, Yamamoto H, Yamamoto M, Hashimoto Y, Oikawa T. Reduction of DNA binding activity of the GATA-1 transcriptional factor in the apoptotic process induced by overexpression of PU.1 in murine erythroleukemia cells. Exp Cell Res. 1998;245:186-194.
18. Muller C, Kowenz-Leutz E, Grieser-Ade S, Graf T, Leutz A. NF-M (chicken C/EBPβ) induces eosinophilic differentiation and apoptosis in a hematopoietic progenitor cell line. EMBO J. 1995;14:6127-6135.
19. Nerlov C, McNagny KM, Döderlein G, Kowenz-Leutz E, Graf T. Distinct C/EBP functions are required for eosinophilic lineage commitment and maturation. Genes Dev. 1998;12:2413-2423.
20. Querfurth E, Schuster M, Kulessa H, et al. Antagonism between C/EBPβ and FOG in eosinophil lineage commitment of multipotent hematopoietic progenitors. Genes Dev. 2000;14:2515-2525.
21. Montecino-Rodriguez E, Leathers H, Dorshkind K. Bipotential B-macrophages progenitors are present in adult bone marrow. Nat Immunol. 2001;2:83-88.
22. Lee C-K, Kim JK, Kim Y, et al. Generation of macrophages from early T progenitors in vitro. J Immunol. 2001;166:5964-5969.
23. Reynaud D, Lefort N, Manie E, Coulombel L, Levy Y. In vitro identification of human pro-B cells that give rise to macrophages, natural killer cells, and T cells. Blood. 2003;101:4313-4321.
24. Mahmud N, Katayama N, Nishii K, et al. Possible involvement of *bcl-2* in regulation of cell-cycle progression of haemopoietic cells by transforming growth factor-β1. Br J Haematol. 1999;105:470-477.
25. Kovacs B, Maus MV, Riley JL, et al. Human CD8+ T cells do not require the polarization of lipid rafts for activation and proliferation. Proc Natl Acad Sci U S A. 2002;99:15006-15011.
26. Ohmine K, Ota J, Ueda M, et al. Characterization of stage progression in chronic myeloid leukemia by DNA microarray with purified hematopoietic stem cells. Oncogene. 2001;20:8249-8257.
27. Makishima H, Ishida F, Ito T, et al. DNA microarray analysis of T cell-type lymphoproliferative disease of granular lymphocytes. Br J Haematol. 2002;118:462-469.
28. Araki H, Katayama N, Mitani H, et al. Efficient *ex vivo* generation of dendritic cells from CD14+ blood monocytes in the presence of human serum albumin for use in clinical vaccine trials. Br J Haematol. 2001;114:681-689.
29. Oda T, Maeda H. A new simple fluorometric assay for phagocytosis. J Immunol Methods. 1986;88:175-183.
30. Metcalf D. Control of granulocytes and macrophages: molecular, cellular, and clinical aspects. Science. 1991;254:529-533.
31. Motoyoshi K. Biological activities and clinical application of M-CSF. Int J Hematol. 1997;67:109-122.
32. Witsell AL, Schook LB. Tumor necrosis factor α is an autocrine growth regulator during macrophage differentiation. Proc Natl Acad Sci U S A. 1992;89:4754-4758.
33. Tracey KJ, Cerami A. Tumor necrosis factor: a pleiotropic cytokine and therapeutic target. Annu Rev Med. 1994;45:491-503.
34. Friedman RM, Vogel SN. Interferons with special emphasis on the immune system. Adv Immunol. 1983;34:97-140.
35. Trinchieri G, Perussia B. Immune interferon: a pleiotropic lymphokine with multiple effects. Immunol Today. 1985;6:131-136.
36. Schreiber RD, Celada A. Molecular characterization of interferon γ as a macrophage activating factor. Lymphokines. 1985;11:87-118.
37. Alon U, Barkai N, Notterman DA, et al. Broad patterns of gene expression revealed by clustering analysis of tumor and normal colon tissues probed by oligonucleotides arrays. Proc Natl Acad Sci U S A. 1999;96:6745-6750.
38. Brons PPT, Raemaekers JMM, Bogman JJT, et al. Cell cycle kinetics in malignant lymphoma studied with in vivo iododeoxyuridine administration, nuclear Ki-67 staining, and flow cytometry. Blood. 1992;80:2336-2343.
39. Jansen JH, Wientjens G-JHM, Fibbe WE, Willemze R, Kluin-Nelemans HC. Inhibition of human macrophage colony formation by interleukin 4. J Exp Med. 1989;170:577-582.
40. Snoeck H-W, Lardon F, Van Bockstaele DR, Peetermans ME. Effects of interleukin-4 (IL4) on myelopoiesis: studies on highly purified CD34+ hematopoietic progenitor cells. Leukemia. 1993;7:625-629.
41. Levesque MC, Haynes BF. Cytokine induction of the ability of human monocyte CD44 to bind hyaluronan is mediated primarily by TNF-α and inhibited by IL-4 and IL-13. J Immunol. 1997;159:6184-6194.
42. Manna SK, Aggarwal BB. Interleukin-4 down-regulates both forms of tumor necrosis factor receptor and receptor-mediated apoptosis, NF-κB, AP-1, and c-Jun N-terminal kinase. J Biol Chem. 1998;273:33333-33341.
43. te Velde AA, Huijbens RJF, de Vries JE, Figdor CG. IL-4 decreases FcγR membrane expression and FcγR-mediated cytotoxic activity of human monocytes. J Immunol. 1990;144:3046-3051.
44. te Velde AA, Huijbens RJF, Heije K, de Vries JE, Figdor CG. Interleukin-4 (IL-4) inhibits secretion of IL-1β, tumor necrosis factor α, and IL-6 by human monocytes. Blood. 1990;76:1392-1397.
45. Snoeck H-W, Lardon F, Lenjou M, Nys G, Van Bockstaele DR, Peetermans ME. Interferon-γ and interleukin-4 reciprocally regulate the production of monocytes/macrophages and neutrophils through a direct effect on committed monopotential bone marrow progenitor cells. Eur J Immunol. 1993;23:1072-1077.
46. Oehler L, Majdic O, Pickl WF, et al. Neutrophil granulocyte-committed cells can be driven to acquire dendritic cell characteristics. J Exp Med. 1998;187:1019-1028.

THE JOURNAL OF BIOLOGICAL CHEMISTRY
© 2004 by The American Society for Biochemistry and Molecular Biology, Inc.

Vol. 279, No. 11, Issue of March 12, pp. 10765–10775, 2004
Printed in U.S.A.

Mutual Regulation of Protein-tyrosine Phosphatase 20 and Protein-tyrosine Kinase Tec Activities by Tyrosine Phosphorylation and Dephosphorylation*

Received for publication, September 22, 2003, and in revised form, December 5, 2003
Published, JBC Papers in Press, December 16, 2003, DOI 10.1074/jbc.M310401200

Naohito Aoki‡§, Shuichi Ueno¶, Hiroyuki Mano¶, Sho Yamasaki‖, Masayuki Shiota, Hitoshi Miyazaki**, Yumiko Yamaguchi-Aoki‡‡, Tsukasa Matsuda‡, and Axel Ullrich‡‡**

*From the ‡Department of Applied Molecular Biosciences, Graduate School of Bioagricultural Sciences, Nagoya University, Furo-cho, Chikusa-ku, Nagoya 464-8601, Japan, ¶Divisions of Functional Genomics, Cardiology and Hematology, Jichi Medical School, Kawachi-gun, Tochigi 329-0498, Japan, ‖Molecular Genetics, Chiba University Graduate School of Medicine, Chiba 260-8670, Japan, **Gene Research Center, University of Tsukuba, Ibaraki 305-8572, Japan, and ‡‡Max Planck Institute for Biochemistry, Department of Molecular Biology, D-82152 Martinsried, Germany*

PTP20, also known as HSCF/protein-tyrosine phosphatase K1/fetal liver phosphatase 1/brain-derived phosphatase 1, is a cytosolic protein-tyrosine phosphatase with currently unknown biological relevance. We have identified that the nonreceptor protein-tyrosine kinase Tec-phosphorylated PTP20 on tyrosines and coimmunoprecipitated with the phosphatase in a phosphotyrosine-dependent manner. The interaction between the two proteins involved the Tec SH2 domain and the C-terminal tyrosine residues Tyr-281, Tyr-303, Tyr-354, and Tyr-381 of PTP20, which were also necessary for tyrosine phosphorylation/dephosphorylation. Association between endogenous PTP20 and Tec was also tyrosine phosphorylation-dependent in the immature B cell line Ramos. Finally, the Tyr-281 residue of PTP20 was shown to be critical for deactivating Tec in Ramos cells upon B cell receptor ligation as well as dephosphorylation and deactivation of Tec and PTP20 itself in transfected COS7 cells. Taken together, PTP20 appears to play a negative role in Tec-mediated signaling, and Tec-PTP20 interaction might represent a negative feedback mechanism.

Protein-tyrosine phosphatases (PTPs)[1] are a large and structurally diverse family of enzymes that catalyze the dephosphorylation of tyrosine-phosphorylated proteins (1, 2). Biochemical and kinetic studies have documented that Cys and an Asp residues in the catalytic domain are essential for the PTP activity. PTPs have been shown to participate as either positive or negative regulators of signaling pathways in a wide range of physiological processes, including cellular growth, differentiation, migration, and survival (1, 2). Despite their important roles in such fundamental cellular processes, the mechanisms by which PTPs exert their effects are largely not understood.

PTP20 (3), which is also known as hematopoietic stem cell fraction (HSCF) (4), PTP-K1 (5), fetal liver phosphatase 1 (6), and brain-derived phosphatase 1 (7), comprises the PEST family of PTPs together with PTP-PEST and PEP PTP and was originally isolated by screening a PC12 cDNA library. Overexpression of PTP20 in PC12 cells results in a more rapid and robust neurite outgrowth in response to nerve growth factor treatment, suggesting that PTP20 is involved in cytoskeletal reorganization (3). Mostly consistent with this observation, overexpression of a dominant negative mutant of fetal liver phosphatase 1 in K562 hematopoietic progenitor cells results in an inhibition of cell spreading and substrate adhesion in response to phorbol ester (6). Recently, through yeast two-hybrid screening the proline, serine, threonine phosphatase-interacting protein (PSTPIP) and PSTPIP2 have been identified to be specific *in vivo* substrates for HSCF, because the phosphotyrosine (Tyr(P)) level of PSTPIP1 is significantly enhanced by coexpression of the catalytically inactive mutant (Cys to Ser) of PTP20 (8, 9). PSTPIP is tyrosine-phosphorylated both in BaF3 cells and in v-Src-transfected COS cells and is shown to be co-localized with the cortical actin cytoskeleton, lamellipodia, and actin-rich cytokinetic cleavage furrow (8), strongly supporting the idea that PTP20/HSCF is a potential regulator of cytokinesis. PSTPIP also interacts with the C-terminal part of the cytosolic protein-tyrosine kinase (PTK) c-Abl, serves as a substrate for c-Abl, and can bridge interactions between c-Abl and PTP20 with the dephosphorylation of c-Abl by PTP20 (10). It has also been reported that PTP20 associates with the negative Src-family kinase regulator Csk via its Src homology 2 (SH2) domain and two putative sites of tyrosine phosphorylation of the phosphatase (11). This association is thought to allow Csk and PTP20 to synergistically inhibit Src-family kinase activity by phosphorylating and dephosphorylating negative and positive regulatory tyrosine residues, respectively.

Regarding post-translational regulation of the PEST family PTPs, it has been documented that phosphorylation of an N-terminal serine residue, which is well conserved in all members of the PEST PTP family, by protein kinase A results in the inhibition of its catalytic activity (12). In addition to proline, serine, and threonine residues in the C-terminal PEST domain of PTP20, a large number of tyrosine residues exist in that region, suggesting the possibility that PTP20 is tyrosine-phosphorylated. Indeed, previous studies reveal that PTP20/HSCF

* This work was supported in part by grants-in-aid for Scientific Research from the Ministry of Education, Science, Sports, and Culture of Japan (to N. A. and T. M.). The costs of publication of this article were defrayed in part by the payment of page charges. This article must therefore be hereby marked "*advertisement*" in accordance with 18 U.S.C. Section 1734 solely to indicate this fact.

§ To whom all correspondence should be addressed: Dept. of Applied Molecular Biosciences, Graduate School of Bioagricultural Sciences, Nagoya University, Furo-cho, Chikusa-ku, Nagoya 464-8601, Japan. Fax: 81-52-789-4128; E-mail: naoki@agr.nagoya-u.ac.jp.

[1] The abbreviations used are: PTP, protein-tyrosine phosphatase; HSCF, hematopoietic stem cell fraction; PSTPIP, proline, serine, threonine phosphatase-interacting protein; PTK, protein-tyrosine kinase; BCR, B cell receptor; SH2, Src homology 2; SH3, Src homology 3; HA, hemagglutinin; GST, glutathione *S*-transferase; WT, wild type; ECL, enhanced chemiluminescence; PH, pleckstrin homology; TH, Tec homology; POV, pervanadate.

becomes tyrosine-phosphorylated by constitutively active forms of Lck and v-Src kinases in transfected cells (8, 11) even though the physiological relevance of tyrosine phosphorylation on PTP20 remains unclear.

In this study we addressed the question of PTP20 regulation with special emphasis on the relevance of tyrosine phosphorylation and its biological impact. Through co-expression with nonreceptor PTKs we found that Tec kinase strongly tyrosine-phosphorylated the catalytically inactive form of PTP20 and that Tec physically interacted with PTP20 in a tyrosine phosphorylation-dependent manner in transfected COS7 cells. Further analyses with a variety of mutants of PTP20 and Tec revealed that C-terminal tyrosine residues of PTP20 and the Tec SH2 domain were necessary in the regulation of respective state of phosphorylation. Ectopic expression of PTP20 in human immature Ramos B cells resulted in suppression of B-cell receptor-induced c-*fos* promoter activity. Moreover, we determined that tyrosine 281 of PTP20 played a role in the dephosphorylation activity of PTP20 against both Tec and PTP20 itself. Our findings suggest a negative feedback mechanism that mutually controls the tyrosine phosphorylation of Tec and PTP20 and regulates Tec activity and B cell receptor (BCR) signaling.

EXPERIMENTAL PROCEDURES

Reagents—Antibodies to hemagglutinin (HA) epitope (Y-11), phosphotyrosine (PY99), glutathione *S*-transferase (GST) (Z-5), Src (SRC2), Lck (2102), JAK2 (M-126), JAK3 (C-21), Csk (C-20), and ZAP70 (LR) were purchased from Santa Cruz Biotechnology Inc. (Santa Cruz, CA). Antibodies to Tec, Itk, Btk, and Bmx were as described previously (13). Antibody to PTP20 was prepared by immunizing rabbits with the N-terminal peptide of PTP20 (MSRQSDLVRSFLEQQEARDH), to which a cysteine residue was added to the C terminus, coupled to keyhole limpet hemocyanin (14). Anti-human IgM antibody $(Fab')_2$ fragment was obtained from Southern Biotechnology Associates (Birmingham, AL). All other reagents were from Sigma unless otherwise noted.

Plasmid Construction—The pSR-based expression vectors for Tec wild-type (WT), Tec kinase mutant, TecY187F, TecY518F, and Tec proteins lacking each subdomain were described previously (15, 16). pEBG plasmids (17) encoding each subdomain of Tec to express the GST-tagged proteins were previously described (18). HA epitope tagging to PTP20 at its N terminus and subsequently all the mutations (cysteine to serine, aspartic acid to alanine, and tyrosine to phenylalanine) in PTP20 were carried out by PCR-based strategy. To express GST-tagged PTP20 in mammalian cells, full-length PTP20 (amino acids 2–453), PTP catalytic domain (amino acids 2–308), and the C-terminal noncatalytic PEST domain (amino acids 271–453) were amplified by PCR and ligated into pEBG vector via the BamHI site. All the plasmids newly constructed were confirmed by sequencing. Expression plasmids for rat Csk and mouse JAK2 were generous gifts from Drs. M. Okada (Osaka University, Japan) and J. N. Ihle (St. Jude Children's Research Hospital, Memphis, TN), respectively. Expression plasmids for mouse Src, Lck, Itk, Btk, Bmx, ZAP-70, and JAK3 were described elsewhere.

Cell Culture and Transfection—COS7 cells were cultured in Dulbecco's modified Eagle's medium (high glucose, Sigma) supplemented with 10% fetal calf serum. Ramos cells (American Type Culture Collection, Manassas, VA) were maintained in RPMI 1640 medium (Invitrogen) supplemented with 10% fetal calf serum. Upon transfection experiments COS7 cells were inoculated at a density of 4×10^5 cells/6-cm dish and grown overnight in Dulbecco's modified Eagle's medium containing 10% fetal calf serum. Expression plasmids were transfected into the cells by the modified calcium phosphate precipitation method (19). After incubation under 3% CO_2, 97% air for 18 h, the transfected cells were washed with phosphate-buffered saline twice and cultured in fresh Dulbecco's modified Eagle's medium containing 10% fetal calf serum for another 24 h under humidified 5% CO_2 and 95% air.

Cell Lysis, Immunoprecipitation, GST Pull-down, and Western Blotting—The transfected cells were lysed with lysis buffer containing 50 mM Tris-HCl (pH 7.5), 5 mM EDTA, 150 mM NaCl, 10 mM sodium phosphate, 10 mM sodium fluoride, 1% Triton X-100, 1 mM phenylmethylsulfonyl fluoride, and 10 μg/ml leupeptin. Lysates were directly subjected to immunoblotting, immunoprecipitation with the indicated antibodies plus protein G- or Protein A-Sepharose beads (Amersham Bioscience), or precipitation with GSH-Sepharose beads (Amersham Bioscience). Proteins in the immunoprecipitates and precipitates were further analyzed by immunoblotting with the indicated antibodies. The protein bands were visualized with an enhanced chemiluminescence (ECL) detection kit (Amersham Bioscience) and light capture system (AE-6962, ATTO, Tokyo, Japan).

c-fos Promoter Assay—Ramos cells (1×10^7/experiment) were subjected to electroporation with 2 μg of the pfos/luc reporter plasmid (20) plus 10 μg of expression plasmids for PTP20 or its mutants. Five hours after transfection cells were incubated for 5 h in the absence or presence of antibodies to human IgM (10 μg/ml). Luciferase activity was measured with the use of the dual luciferase assay system (Promega, Madison, WI).

RESULTS

Tec Is a Potent Regulator of PTP20—Although PTP20 has been shown to be a substrate of v-Src (8) and constitutively active Lck (11), the physiological relevance of PTP20 tyrosine phosphorylation remains unknown. Northern blot analysis revealed that PTP20 was abundantly expressed in spleen, suggesting a role in the immune system (data not shown). Therefore, it was reasoned that other PTKs of immune cells might be involved in PTP20 regulation by tyrosine phosphorylation. To examine this possibility HA-tagged PTP20 was co-expressed with various cytosolic PTKs including Src and Lck in COS7 cells. We used a catalytically inactive form of PTP20 for this experiment because autodephosphorylation activity of PTP20 has been previously reported (8). Cells were lysed, PTP20 was immunoprecipitated with anti-HA antibody, and the immune complexes were subjected to SDS-PAGE and immunoblotting with anti-phosphotyrosine antibody. As shown in Fig. 1*A*, PTP20 was tyrosine-phosphorylated by Src and Lck and co-immunoprecipitated with proteins with 56 and 60 kDa, likely corresponding to Lck and Src, respectively. In the case of ectopic Lck expression, endogenous Src seemed to be included in the immune complex, as suggested by the presence of a 66-kDa phosphotyrosine-containing band. PTP20 was slightly tyrosine-phosphorylated by Csk and co-immunoprecipitated with a faintly tyrosine-phosphorylated 70-kDa band, which seemed unlikely to be Csk. JAK2 but not JAK3 also tyrosine-phosphorylated PTP20 and appeared to be co-immunoprecipitated with PTP20. Most notably, PTP20 was strongly tyrosine-phosphorylated by Tec and co-immunoprecipitated with a heavily tyrosine-phosphorylated protein of 74 kDa and other minor proteins of 120 and 35 kDa. Based on the molecular mass, the 74-kDa protein was likely to represent Tec. Itk, another member of Tec/Btk family, also tyrosine-phosphorylated PTP20 to a lesser extent and was co-immunoprecipitated, whereas related PTKs Btk and Bmx did not tyrosine phosphorylate PTP20 and were not co-immunoprecipitated. Because all the transfected PTKs were obviously expressed as compared with mock transfectant (Fig. 1, *panel B*), it was suggested that Tec tyrosine-phosphorylated PTP20 with the greatest efficiency.

Tec Is a Potential Substrate of PTP20—To examine the relationship between PTP20 and Tec in more detail, Tec was co-transfected with WT or a catalytically inactive C/S form of PTP20 into COS7 cells, and either PTP20 or Tec was immunoprecipitated followed by immunoblotting with anti-phosphotyrosine antibody. When HA-PTP20 WT was expressed, no phosphorylated bands were visible in both anti-HA and anti-Tec immunoprecipitates, possibly due to dephosphorylation activity of PTP20 against both Tec and itself (Fig. 2). Two major bands with 74 and 50 kDa in the anti-HA and anti-Tec immune complexes were detected with anti-phosphotyrosine antibody only when the PTP20 C/S mutant was co-transfected with Tec. Reprobing with anti-Tec and anti-HA antibodies clearly revealed that the bands represent Tec and HA-PTP20. No phosphorylation of Tec was observed when Tec alone was introduced into COS7 cells, suggesting that the interaction between Tec and PTP20 was required for Tec phosphorylation and pos-

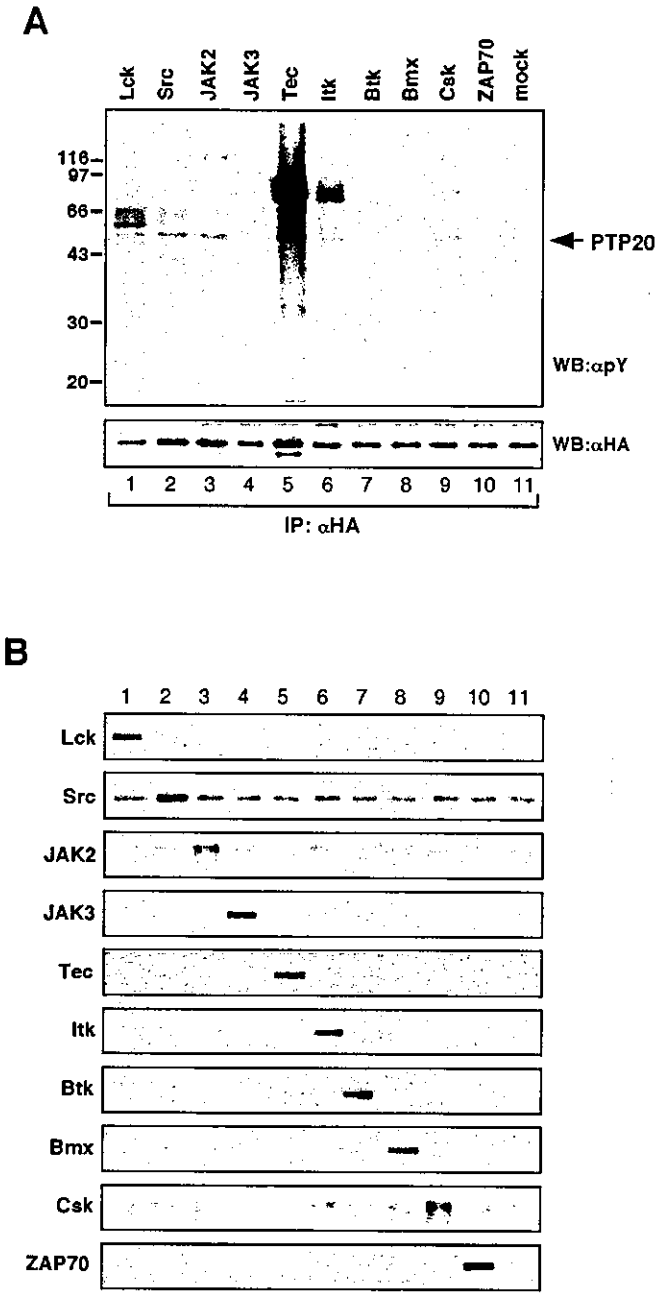

FIG. 1. **Tyrosine phosphorylation of PTP20 by various PTKs.** *A*, COS7 cells were transiently transfected with HA-PTP20 C/S together with either Lck, Src, JAK2, JAK3, Tec, Itk, Btk, Bmx, Csk, or ZAP70. Cells were lysed, and PTP20 was immunoprecipitated (*IP*) with anti-HA antibody followed by immunoblotting (*WB*) with anti-phosphotyrosine antibody (PY99 (*αpY*)). The same membrane was reprobed with anti-HA antibody after stripping. *B*, an aliquot of the cell lysates was immunoblotted with the indicated antibodies to confirm substantial expression of each PTK.

sibly activation. These results suggest that PTP20 is a substrate of Tec and that Tec is also a substrate of PTP20.

Phosphotyrosine-dependent Interaction between PTP20 and Tec—Tec is composed of several distinct domains including pleckstrin homology (*PH*), Tec homology (*TH*), SH3, SH2, and kinase (*KD*) domains (Fig. 3, *panel A*). All of these domains are necessary for full function of Tec under physiological conditions (15, 16). To examine which domains are involved in interaction with PTP20, Tec mutants each lacking one of the domains were co-transfected with the catalytically inactive form of PTP20 into COS7 cells. A kinase mutant as well as two mutants (Y187F and Y518F) where tyrosine residues were replaced by phenylalanines were also included. Cells were lysed, and PTP20 was immunoprecipitated followed by immunoblotting with anti-phosphotyrosine antibody. PTP20 was tyrosine-phosphorylated by the Y187F mutant as well as mutants lacking PH, TH, and SH3 domains to a similar extent as compared with Tec WT (Fig. 3, *panel B*). As expected, the Y518F mutant, which is missing the autophosphorylation site for Tec activation, and the inactive mutant of a kinase mutant could not tyrosine phosphorylate PTP20. Interestingly, the ΔPH mutant could tyrosine phosphorylate PTP20 but was not co-immunoprecipitated with PTP20. Most strikingly, the ΔSH2 mutant could not tyrosine phosphorylate PTP20 and was not co-immunoprecipitated with PTP20. When a membrane on which aliquots of total cell lysates were blotted was probed with anti-phosphotyrosine antibody, it was revealed that co-expression of the Tec ΔSH2 mutant and PTP20 resulted in no tyrosine phosphorylation on both molecules and that the Tec ΔPH mutant tyrosine-phosphorylated (Fig. 3, *panel C*). Tec SH2 domain-dependent interaction with PTP20 was further investigated by co-transfecting the PTP20 C/S mutant with plasmids encoding GST fusion proteins of Tec domains in the presence or absence of Tec into COS7 cells. Cell lysates were subjected to pull-down experiments with GSH-Sepharose beads. Precipitates were separated by SDS-PAGE followed by immunoblotting with the indicated antibodies. In the absence of full-length Tec co-expression, no substantial binding of PTP20 to any of the Tec domains was apparent (Fig. 3, *panel D*). In contrast, in the presence of full-length Tec, phosphorylated PTP20 bound to only the SH2 domain of Tec. Given that co-expression of Tec should result in marked tyrosine phosphorylation of PTP20 in COS7 cells, these data indicate that the PTP20-Tec interaction is mediated predominantly by the SH2 domain of Tec and phosphotyrosine residues of PTP20.

Next, we tried to identify the binding site(s) for Tec in PTP20. Because the interaction of Tec with PTP20 was mediated by the Tec SH2 domain, potential tyrosine residues of phosphorylation were first taken into consideration. There are 13 tyrosine residues (Tyr-62, Tyr-68, Tyr-86, Tyr-101, Tyr-144, Tyr-192, Tyr-244, Tyr-281, Tyr-285, Tyr-303, Tyr-354, Tyr-381, Tyr-419) in the PTP20 sequence, and all the residues are perfectly conserved among human and mouse orthologs (Fig. 4). We focused our attention on the tyrosine residues Tyr-281, Tyr-285, Tyr-303, Tyr-354, Tyr-381, and Tyr-419 located in the C-terminal PEST domain of PTP20, and 6 residues were individually mutated.

First, the mutants were tested for the extent of tyrosine phosphorylation by Tec in transfected COS7 cells. Total cell lysates were subjected to anti-phosphotyrosine blotting. Fig. 5, *panel A*, demonstrates that the PTP20 mutants (Y281F, Y303F, Y354F, Y381F) in which Tyr-281, Tyr-303, Tyr-354, and Tyr-381 were individually mutated exhibited dramatic reduction in tyrosine phosphorylation levels, whereas no apparent reduction for Y285F and Y419F was observed. Combinational mutation of Tyr-281, Tyr-303, Tyr-354, and Tyr-381 totally abolished tyrosine phosphorylation of PTP20. In keeping with these data, anti-phosphotyrosine blotting also demonstrated that tyrosine phosphorylation of Tec was concomitantly reduced. This observation was further extended by GST pull-down experiments using the Tec SH2 domain. COS7 cells were then transfected with PTP20 YF variants together with Tec and Tec-Tec SH2, as outlined in Fig. 3, *panel C*. Mutation of either Tyr-281, Tyr-303, Tyr-354, or Tyr-381 of PTP20 resulted in reduced binding capacity of PTP20 to the Tec SH2 domain, and again, such binding was completely abrogated by substituting all the tyrosine residues (Fig. 5, *panel B*). Together these data clearly indicate that four tyrosine residues in the C-ter-

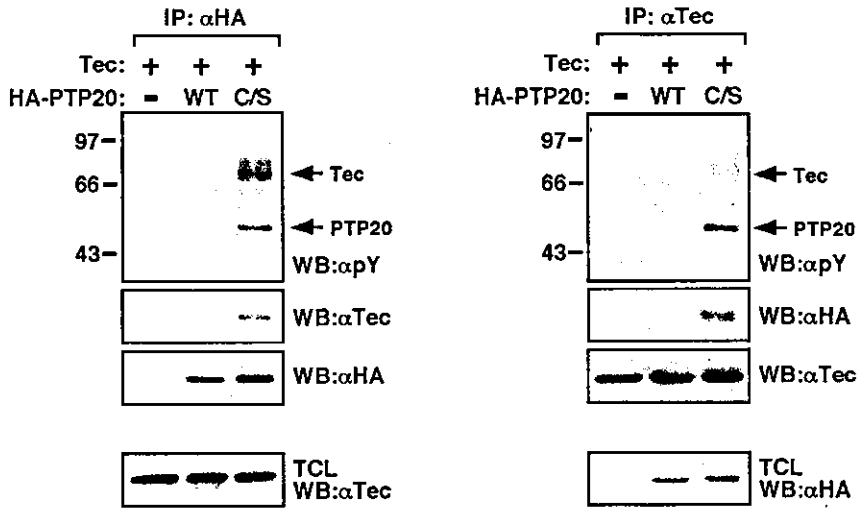

FIG. 2. **Tyrosine phosphorylation-dependent interaction of PTP20 with Tec.** Tec cDNA was transiently introduced into COS7 cells together with either empty vector (mock), HA-PTP20 WT, or C/S and lysed. PTP20 or Tec was immunoprecipitated either with anti-HA (*left panels*) or anti-Tec (*right panels*) antibody, respectively. The immunoprecipitates (*IP*) were separated by SDS-PAGE followed by immunoblotting (*WB*) sequentially with the indicated antibodies. The bands corresponding to Tec and PTP20 are indicated by *arrows*. In either case expression of Tec or HA-PTP20 was confirmed using aliquots of total cell lysates (*TCL*) by immunoblotting (*lowest panels*). *αpY*, anti-phosphotyrosine antibody.

minal non-catalytic region of PTP20 are involved in not only binding to the Tec SH2 domain but also in the phosphorylation and subsequent activation of Tec.

We asked whether the C-terminal non-catalytic region of PTP20 was enough for phosphorylation and activation of Tec. To this end, PTP20 deletion mutants lacking either an N-terminal catalytic or a C-terminal non-catalytic segment were made, but the resultant constructs could not be expressed in COS7 cells, although comparable amounts of transcripts were detected (data not shown). To solve this problem, the N-terminal PTP domain and the C-terminal PEST domain were inserted into pEBG vector and were expressed as GST fusion proteins in COS7 cells. These pEBG plasmids encoding the PTP domain and full length of PTP20 C/S mutant and the PEST domain of PTP20 were co-transfected into COS7 together with Tec. Anti-phosphotyrosine blotting documented that Tec was highly tyrosine-phosphorylated with the full-length but not the PTP domain of the PTP20 C/S mutant (Fig. 6, *panel A*), supporting previous data shown in Fig. 5, where the C-terminal part of PTP20 was essential for tyrosine phosphorylation of Tec. Interestingly, the presence of the PEST domain of PTP20 caused tyrosine phosphorylation of PTP20, but the extent was lower than in the presence of the full-length PTP20 C/S mutant. Equivalent expression of each construct was confirmed by Western blotting with anti-Tec and anti-GST antibodies. To further examine the involvement of the PEST domain, lysates were precipitated with GSH-Sepharose beads followed by immunoblotting with anti-phosphotyrosine antibody. A phosphorylated 74-kDa band, which was shown to be Tec by immunoblotting, was co-precipitated with full-length PTP20 C/S mutant, whereas the PTP domain alone could not capture Tec (Fig. 6, *panel B*). A faint tyrosine-phosphorylated band with the same mobility of 74 kDa that co-precipitated with the PEST domain appeared to be Tec but could not be detected by our anti-Tec antibody presumably due to sensitivity. These results suggest that the PEST domain of PTP20 is necessary but not sufficient for not only hyperphosphorylation and activation of, but also association with Tec.

Negative Regulatory Roles of PTP20 in BCR Signaling—All the experiments documented above were conducted in transfected COS7 cells. To demonstrate a physiological relevance of the PTP20-Tec interaction, evidence of such an association in non-transfected cells was required. To this end we selected human Ramos immature B cells, because it has been reported that they express relatively high amounts of endogenous Tec (21). As shown above, interaction of PTP20 with Tec is mediated by tyrosine phosphorylation of PTP20, and PTP20 has autodephosphorylation activity, implying that it would be difficult to detect a phosphotyrosine-dependent interaction of PTP20 with other molecules including Tec endogenously. To overcome this experimental difficulty, protein-tyrosine phosphorylation was induced in Ramos cells by treatment with pervanadate (POV). Cells were starved for 16 h in serum-free medium and then either left unstimulated or treated with 0.1 mM POV for 30 min and lysed. Cell lysates were immunoprecipitated with either anti-phosphotyrosine antibody or anti-Tec antibody. Our PTP20-specific antibody could not be used due to its inability in immunoprecipitation experiments. In anti-phosphotyrosine immunoprecipitates, specific bands with 74 and 50 kDa corresponding to human Tec and PTP20 were detected only upon POV treatment (Fig. 7). A tyrosine-phosphorylated band with 50 kDa in the anti-Tec immunoprecipitates was readily detected by the anti-PTP20 antibody but only when cells received POV pretreatment (Fig. 7). These results indicate that endogenous Tec and PTP20 interact with each other in a phosphotyrosine-dependent manner in Ramos B cells.

Although upstream regulators such as cytokine receptors, lymphocyte surface antigens, G protein-coupled receptors, receptor type PTKs, or integrins for Tec in blood cells including Ramos B cells have been relatively well investigated (13, 20, 22–26), only limited information regarding downstream regulators of Tec has been available so far. If the data obtained in transfected COS7 cells are true, PTP20 would be thought to play a negative regulatory role in Tec-mediated signaling. To examine this, either the PTP20 WT, the inactive C/S mutant, or another form of catalytically inactive mutant D/A was transiently co-transfected with the pfos/luc reporter plasmid into Ramos cells, because the promoter of the c-*fos* proto-oncogene is activated in response to BCR cross-linking in the cells. Cells were either left unstimulated or treated with anti-human IgM $F(ab')_2$ fragments for 5 h. Cell lysates were assayed for luciferase activity. BCR cross-linking induced a marked activation of the c-*fos* promoter (Fig. 8). Expression of PTP20 WT totally inhibited BCR-induced activation of the c-*fos* promoter as well as its basal activity, whereas only about 20% inhibition of the promoter activation was observed in the co-expression of catalytically inactive forms of PTP20, strongly indicating that PTP20 is a negative regulator of BCR-Tec-c-*fos* signaling.

Tyrosine Phosphorylation of PTP20 by Tec Modulates Its Catalytic Activity against Tec as Well as Itself—We demonstrated that specific tyrosine residues Tyr-281, Tyr-303, Tyr-354, and Tyr-381 of PTP20 could be phosphorylated by Tec and served as Tec binding sites (Fig. 5). To further investigate physiological relevance of PTP20 tyrosine phosphorylation, substitution of the tyrosine residues with phenylalanine in PTP20 WT was performed. The YF mutants of HA-PTP20 WT

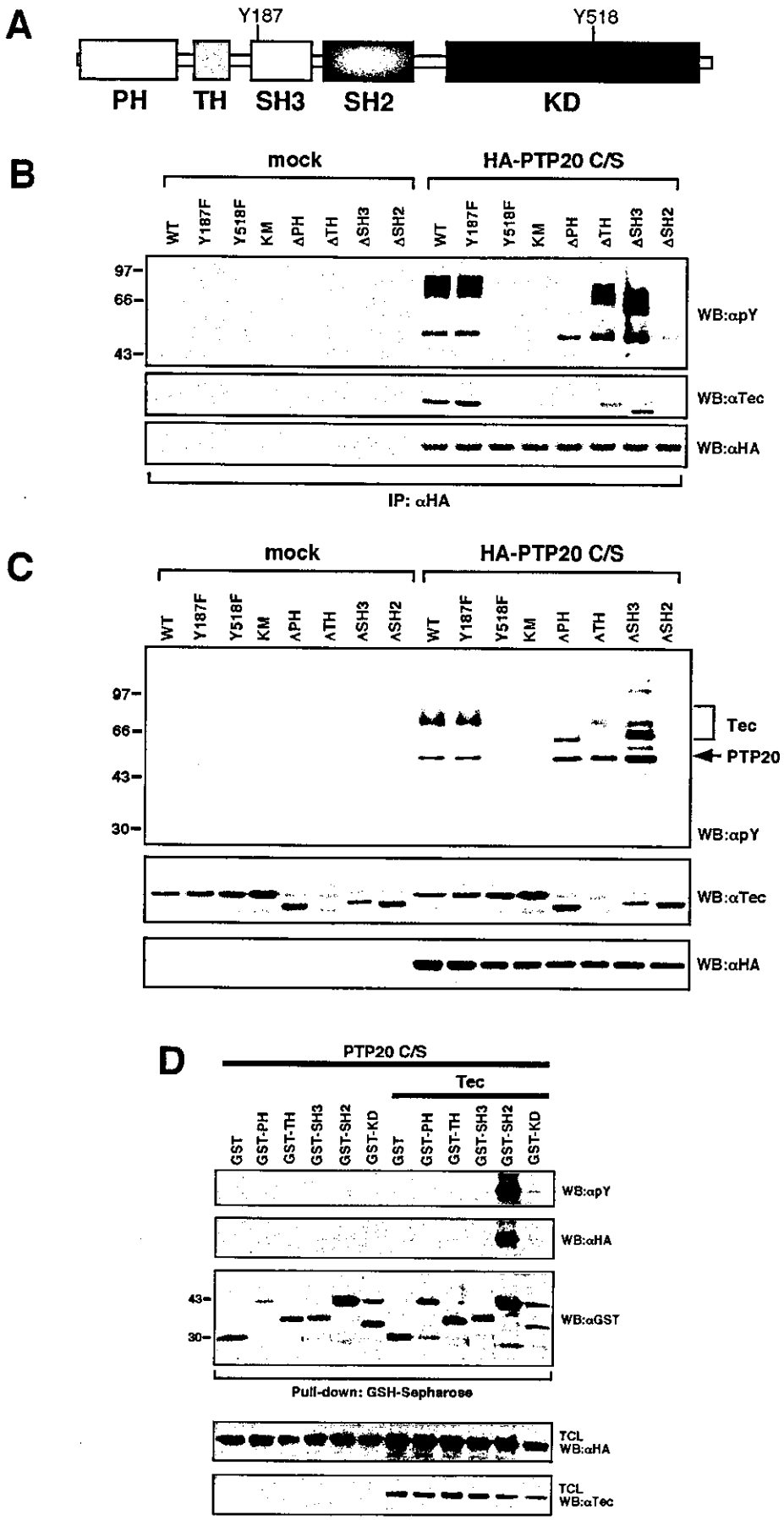

FIG. 3. **Tec SH2 domain is essential for both tyrosine phosphorylation of PTP20 and association of Tec with PTP20.** *A*, schematic organization of mouse Tec into PH, TH, SH3, SH2, and kinase (*KD*) domains. *B*, COS7 cells were transiently transfected with either empty vector (*mock*) or HA-PTP20 C/S together with the indicated Tec mutants. Cells were lysed, and HA-PTP20 was immunoprecipitated (*IP*) followed by immunoblotting (*IB*) with anti-phosphotyrosine antibody (PY99 (*αpY*)). The same membrane was sequentially reprobed with anti-Tec and anti-HA antibodies after stripping. *C*, aliquots of the total cell lysates (*TCL*) were separated by SDS-PAGE followed by immunoblotting with indicated antibodies. *D*, COS7 cells were transiently transfected with pEBG empty vector (GST) or bearing each of Tec domains (PH, TH, SH3, SH2, and KD) in the absence or presence of Tec plasmid. Cells were lysed, and GST fusion proteins were precipitated by GSH-Sepharose beads followed by immunoblot analysis with anti-phosphotyrosine (*pY*) antibody. The same membrane was sequentially reprobed with indicated antibodies. Expression of PTP20 and Tec was confirmed using aliquots of total cell lysates (*TCL*) by immunoblotting as indicated.

```
PTP20(rat)   MSRQSDLVRS FLEQQEARDH RKGAILAREF SDIKARSVAW KTEGVCSTKA GSQQGNSKKN  60
HSCF(mouse)  MSRHTDLVRS FLEQLEARDY REGAILAREF SDIKARSVAW KSEGVCSTKA GSRLGNTNKN  60
BDP1(human)  MSRSLDSARS FLERLEARGG REGAVLAGEF SDIQACSAAW KADGVCSTVA GSRPENVRKN  60

                62     68                    86                  101
PTP20(rat)   RYKDVVPYDE TRVILSLLQE EGHGDYINAN FIRGTDGSQA YIATQGPLPH TLLDFWRLVW 120
HSCF(mouse)  RYKDVVAYDE TRVILSLLQE EGHGDYINAN FIRGIDGSQA YIATQGPLPH TLLDFWRLVW 120
BDP1(human)  RYKDVLPYDQ TRVILSLLQE EGHSDYINGN FIRGVDGSLA YIATQGPLPH TLLDFWRLVW 120

                                   144
PTP20(rat)   EFGIKVILMA CQETENGRRK CERYWAQERE PLQAGPFCIT LTKETALTSD ITLRTLQVTF 180
HSCF(mouse)  EFGVKVILMA CQETENGRRK CERYWAREQE PLKAGPFCIT LTKETTLNAD ITLRTLQVTF 180
BDP1(human)  EFGVKVILMA CREIENGRKR CERYWAQEQE PLQTGLFCIT LIKEKWLNED IMLRTLKVTF 180

                         192
PTP20(rat)   QKESRPVHQL QYMSWPDHGV PSSSDHILTM VEEARCLQGL GPGPLCVHCS AGCGRTGVLC 240
HSCF(mouse)  QKEFRSVHQL QYMSWPDHGV PSSSDHILTM VEEARCLQGL GPGPLCVHCS AGCGRTGVLC 240
BDP1(human)  QKESRSVYQL QYMSWPDRGV PSSPDHMLAM VEEARRLQGS GPEPLCVHCS AGCGRTGVLC 240

                244                                    281 285
PTP20(rat)   AVDYVRQLLL TQTIPPNFSL FEVVLEMRKQ RPAAVQTEEQ YRFLYHTVAQ LFSRTLQNNS 300
HSCF(mouse)  AVDYVRQLLL TQTIPPNFSL FQVVLEMRKQ RPAAVQTEEQ YRFLYHTVAQ LFSRTLQDTS 300
BDP1(human)  TVDYVRQLLL TQMIPPDFSL FDVVLKMRKQ RPAAVQTEEQ YRFLYHTVAQ MFCSTLQNAS 300

                303                                                  354
PTP20(rat)   PLYQNLKENR APICKDSSSL RTSSALPATS RPLGGVLRSI SVPGPPTLPM ADTYAVVQKR 360
HSCF(mouse)  PHYQNLKENC APICKEAFSL RTSSALPATS RPPGGVLRSI SVPAPPTLPM ADTYAVVQKR 360
BDP1(human)  PHYQNIKENC APLYDDALFL RTPQALLAIP RPPGGVLRSI SVPGSPGHAM ADTYAVVQKR 360

                                   381
PTP20(rat)   GASGSTGPGT RAPNST---- --DTPIYSQV APRIQRPVSH TENAQGTTAL GRVPADENPS 414
HSCF(mouse)  GASAGTGPGP RAPTST---- --DTPIYSQV APRAQRPVAH TEDAQGTTAL RRVPADQNSS 414
BDP1(human)  GAPAGAGSGT QTGTGTGARS AEEAPLYSKV TPRAQRPGAH AEDARGTLP- GRVPADQSPA 420

                419
PTP20(rat)   GPDAYEEVTD GAQTGGLGFN LRIGRPKGPR DPPAEWTRV 453
HSCF(mouse)  GPDAYEEVTD GAQTGGLGFN LRIGRPKGPR DPPAEWTRV 453
BDP1(human)  GSGAYEDVAG GAQTGGLGFN LRIGRPKGPR DPPAEWTRV 458
```

FIG. 4. **Sequence alignment of PTP20 with its human (brain-derived phosphatase 1 (*BDP1*)) and mouse (*HSCF*) orthologs.** The 13 conserved tyrosine residues are *boxed* and *numbered* based on the amino acid sequence of PTP20. PTP catalytic domains are indicated by *gray shading*.

were co-transfected with Tec and the PTP20 C/S mutant without epitope tagging, and effects on the extent of tyrosine phosphorylation on Tec were analyzed by anti-phosphotyrosine blotting. As shown in Fig. 9*A*, substitution of Tyr-281 with phenylalanine (Y281F) resulted in dramatic loss of PTP20 dephosphorylation activity against Tec. On the other hand, Tec could be dephosphorylated by Y303F, Y354F, and Y381F to nearly the same extent by PTP20 WT. The PTP20 Y281F/Y303F/Y354/F381F mutant in which 4 tyrosine residues were substituted by phenylalanine also exhibited apparently no dephosphorylation activity against Tec. Equivalent expression of HA-PTP20 was confirmed by immunoblotting (*lowest panel*). Next, the autodephosphorylation activity of the YF mutants of HA-PTP20 WT was assessed by co-transfecting Tec and-PEST encoding the GST-PTP20 PEST domain into COS7 cells, as GST-PTP20 PEST alone became tyrosine-phosphorylated in the presence of Tec (Fig. 6). Cells were lysed and GST-PTP20 PEST was precipitated with GSH-Sepharose beads followed by anti-phosphotyrosine blotting. Again, PTP20 Y281F as well as PTP20 Y281F/Y303F/Y354/F381F showed no dephosphorylation activity against GST-PTP20 PEST, whereas PTP20 Y303F, Y354F, and Y381F as well as PTP20 WT could dephosphorylate GST-PTP20 PEST (Fig. 9*B*). These YF mutants also were transfected into Ramos B cells, and c-*fos* promoter activity was assayed after BCR ligation. Ectopic expression of PTP20 Y281F and Y281F/Y303F/Y354/F381F mutants still inhibited c-*fos* promoter activity (about 50%, relative to mock transfectants), but the extent was significantly lower than that of WT as well as other YF mutants. These results strongly suggest that phosphorylation of Tyr-281 on PTP20 is essential for expression of catalytic activity against not only Tec but also PTP20 itself in transfected COS7 cells as well as in Ramos B cells, although other tyrosine residues, Tyr-303, Tyr-354, and Tyr-381, are also phosphorylated by Tec.

DISCUSSION

Many signaling pathways triggered by PTKs can be potentially modulated by PTPs in a negative or positive manner under cellular context. In some cases phosphorylation on the tyrosine residues of PTPs themselves can modulate their catalytic activities. For example, SH2 domain-containing PTP SHP-2 is tyrosine-phosphorylated upon stimulation by a variety of growth factors (27–29) and cytokines (30–35). Once SHP-2 becomes tyrosine-phosphorylated, their catalytic activity might be increased and modulated its own tyrosine phosphorylation level by autodephosphorylation activity (36, 37). It also has been reported that tyrosine phosphorylation of PTP1B upon insulin and epidermal growth factor treatment causes reduction in its catalytic activity, thereby enhancing apparent insulin receptor- and epidermal growth factor receptor-mediated signaling pathways (38, 39). Thus, tyrosine phosphorylation of PTPs appeared to be critical for the regulation of their biological functions.

Among the PEST family PTPs, PTP20 is an only member that gets phosphorylated on tyrosine residues, whereas no tyrosine phosphorylation of other members, PTP-PEST and PTP-

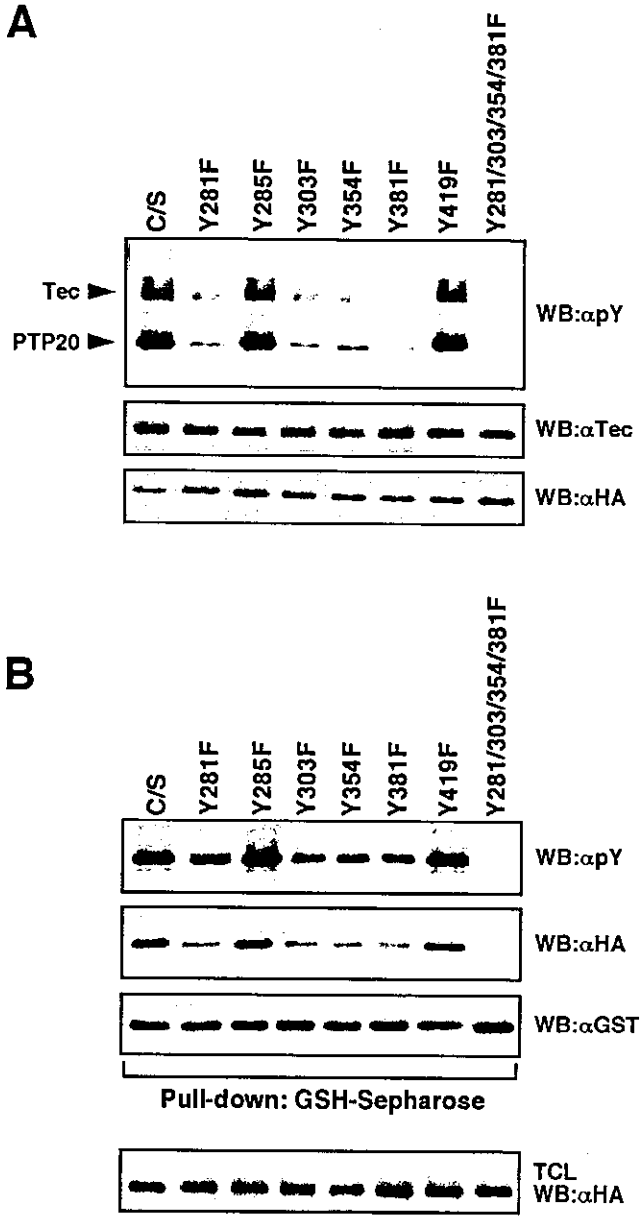

FIG. 5. **Specific tyrosine residues of PTP20 are necessary for tyrosine phosphorylation of Tec and association with Tec SH2 domain.** *A*, HA-PTP20 C/S or its YF (tyrosine to phenylalanine substitution) mutants as indicated were co-transfected into COS7 cells with Tec. Aliquots of total cell lysates (*TCL*) were immunoblotted (*WB*) with anti-phosphotyrosine (*αpY*) antibody. The same membrane was sequentially reprobed with anti-Tec and -HA antibodies. *B*, COS7 cells were co-transfected with expression plasmids for HA-PTP20 C/S or its YF mutants, Tec, and GST-Tec-SH2 domain. Cells were lysed, and GST-Tec-SH2 domain was precipitated with GSH-Sepharose beads followed by immunoblot analysis by sequential probing with anti-phosphotyrosine, anti-HA, and anti-GST antibodies. Expression of nearly the same amounts of PTP20 was confirmed by immunoblotting of aliquots of total cell lysates with anti-HA antibody.

PEP, has been reported. In the present study, we clearly demonstrated that PTP20 was tyrosine-phosphorylated by a cytosolic Tec kinase. As previously reported for phosphorylation of PTP20 by constitutively active Src family kinases (8, 11), the catalytically inactive form of PTP20 was found to be tyrosine-phosphorylated to a greater extent by Tec, whereas apparently no phosphorylation on PTP20 WT was obvious, possibly due to its autodephosphorylation activity. Src and Lck indeed tyrosine-phosphorylated PTP20, but the extent of tyrosine phosphorylation of PTP20 by Tec was shown to be the greatest (Fig. 1). Moreover, related Itk did tyrosine-phosphorylate PTP20 to a lesser extent, but Btk and Bmx did not (Fig. 1). These results suggest that Tec kinase tyrosine phosphorylates PTP20 more specifically and preferentially than Src family kinases and its related kinases do.

Without ectopic PTP20 expression, tyrosine phosphorylation of Tec kinase was not detected in transfected COS7 cells (Fig. 2). Although co-expression of PTP20 WT did not induce tyrosine phosphorylation of Tec, the catalytically inactive C/S variant of PTP20 caused tyrosine phosphorylation of Tec and co-immunoprecipitated with Tec. These results strongly suggest that a dominant-negative effect of PTP20 C/S expression on Tec tyrosine phosphorylation seems to be unlikely and, rather, that Tec was possibly autophosphorylated and further activated by interacting with PTP20 and then was immediately dephosphorylated and deactivated by PTP20, which might also be activated through interaction with Tec in a tyrosine phosphorylation-dependent manner. A deletion of the Tec SH2 domain abrogated tyrosine phosphorylation of Tec as well as PTP20 and association between Tec and PTP20 (Fig. 3). Likewise, substitution of individual tyrosine residues Tyr-281, Tyr-303, Tyr-354, and Tyr-381 with phenylalanines of PTP20 reduced not only tyrosine phosphorylation of Tec and PTP20 itself but also association of PTP20 with the Tec SH2 domain (Fig. 5). Substitution of all the four tyrosine residues (Fig. 5) as well as a deletion of the C-terminal non-catalytic segment (Fig. 6) completely abolished those events, and the C-terminal segment alone partially induced Tec tyrosine phosphorylation (Fig. 6), supporting the idea that phosphotyrosine-dependent interaction between PTP20 and Tec is essential for determining a mutual state of phosphorylation and activation. Taken together, we propose a working hypothesis of tyrosine phosphorylation-dependent interaction between PTP20 and Tec kinase (Fig. 10).

PTPs exhibit elaborate substrate specificity *in vivo*. This specificity can be achieved at two levels. First, the phosphatase catalytic domain itself displays an intrinsic specificity for its substrate. However, the affinity between the catalytic domain and its substrate is often low. Actually, the PTP domain of the catalytically inactive PTP20 alone could not capture a potential substrate Tec kinase (Fig. 6). A further enhancement of the specificity is achieved by protein-protein targeting; the Tec SH2 domain and phosphorylated tyrosine residues on PTP20 could enhance the interaction between the two molecules. In Ramos B cells, we could detect tyrosine phosphorylation-dependent interaction between PTP20 and Tec only when cells were treated with pervanadate (Fig. 7). In this case, however, apparent binding might have resulted from a sole interaction of phosphorylated tyrosines of PTP20 C-terminal with the Tec SH2 domain and, therefore, underestimated because vanadate can get into the catalytic pocket of PTP20 reversibly and inhibit interaction between the PTP domain segment of PTP20 and tyrosine-phosphorylated Tec kinase. Upon physiological stimulation both PTP20 catalytic domain-Tec phosphotyrosine(s) and PTP20 phosphotyrosine-Tec SH2 domain bindings could play an essential role.

Most interestingly, tyrosine phosphorylation of PTP20 appears to regulate its catalytic activity against Tec and PTP20 itself. Among the tyrosine residues phosphorylated by Tec kinase, tyrosine 281 might be critical for dephosphorylation activity of PTP20 in transfected COS7 cells as well as in Ramos B cells (Fig. 9). In the case of ectopic expression in COS7 cells, substitution of the Tyr-281 nearly abolished dephosphorylation activity against both PTP20 and Tec (Fig. 9, *A* and *B*). On the other hand Y281F as well as Y281F/Y303F/Y354/F381F mutants exhibited reduced, but still ~50% dephosphorylation activity as compared with mock transfectants when expressed in

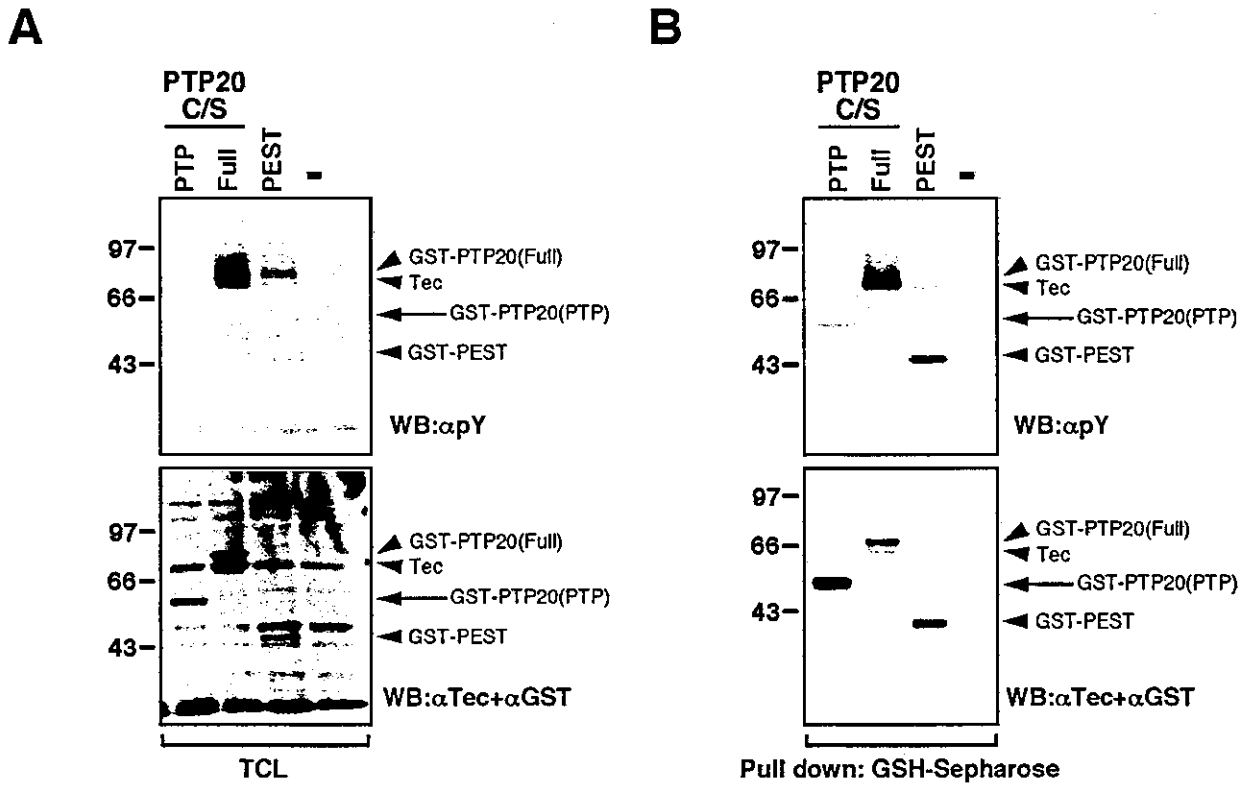

FIG. 6. **Both PTP catalytic and PEST domains of PTP20 are involved in maximal phosphorylation of Tec and association with Tec.** Tec was co-transfected with either empty pEBG vector (−) or that bearing the PTP20 catalytic domain (*PTP*), full-length PTP20 (*Full*), or the non-catalytic PEST domain of PTP20 (*PEST*). *A*, aliquots of total cell lysates (*TCL*) were subjected to immunoblotting with anti-phosphotyrosine antibody (*αpY, upper panel*). The same membrane was reprobed with a mixture of anti-Tec and anti-GST antibodies. *B*, remaining cell lysates were precipitated with GSH-Sepharose beads and processed as mentioned above. The bands corresponding to individual products are indicated by *arrows*.

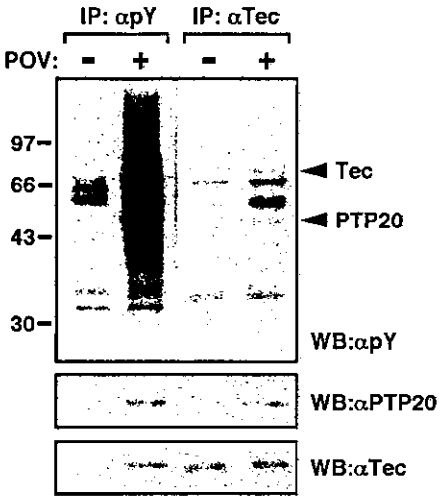

FIG. 7. **Tyrosine phosphorylation-dependent interaction of endogenous PTP20 with endogenous Tec in Ramos B cells.** Ramos cells were treated with 0.1 mM POV for 15 min at 37 °C, lysed, and subjected to immunoprecipitation with either anti-phosphotyrosine (*αpY*) or anti-Tec antibody. The immunoprecipitates (*IP*) were immunoblotted (*WB*) by anti-phosphotyrosine antibody. The same membranes were sequentially reprobed with anti-PTP20 and -Tec antibodies. The bands corresponding to Tec and PTP20 are indicated by *arrowheads*.

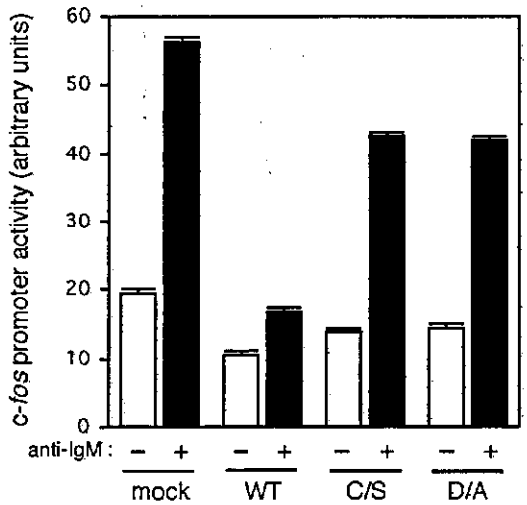

FIG. 8. **Negative role of PTP20 in BCR signaling.** Ramos cells (1×10^7) were subjected to electroporation with 2 μg of the pfos/luc reporter plasmid together with 10 μg of pcDNA3 vector (mock) or bearing PTP20 WT, C/S, or D/A mutant. Five hours after transfection cells were incubated for an additional 5 h in the absence (*open bars*) or presence (*closed bars*) of anti-IgM (ab') (10 μg/ml). Cells lysates were then assayed for luciferase activity. Data are expressed as mean ± S.D. of triplicate determinations.

Ramos B cells (Fig. 9*C*), suggesting that other direct or indirect mechanisms to regulate PTP20 activity are involved in dephosphorylation and deactivation of Tec in the cells. However, we cannot exclude the possibility that phosphorylation on serine and threonine residues rich in the C-terminal region of PTP20 might affect catalytic activity of PTP20, as PTP20 can be regulated under the control of follicle-stimulating hormone in rat ovarian granulosa cells, where no tyrosine phosphorylation on PTP20 was observed (14).

It has been reported that constitutively active Lck phosphorylates tyrosine residues 354 and 381 on PTP20, which are in turn recognized by the Csk SH2 domain (11). In that report it was also documented that mutation of both the tyrosine resi-

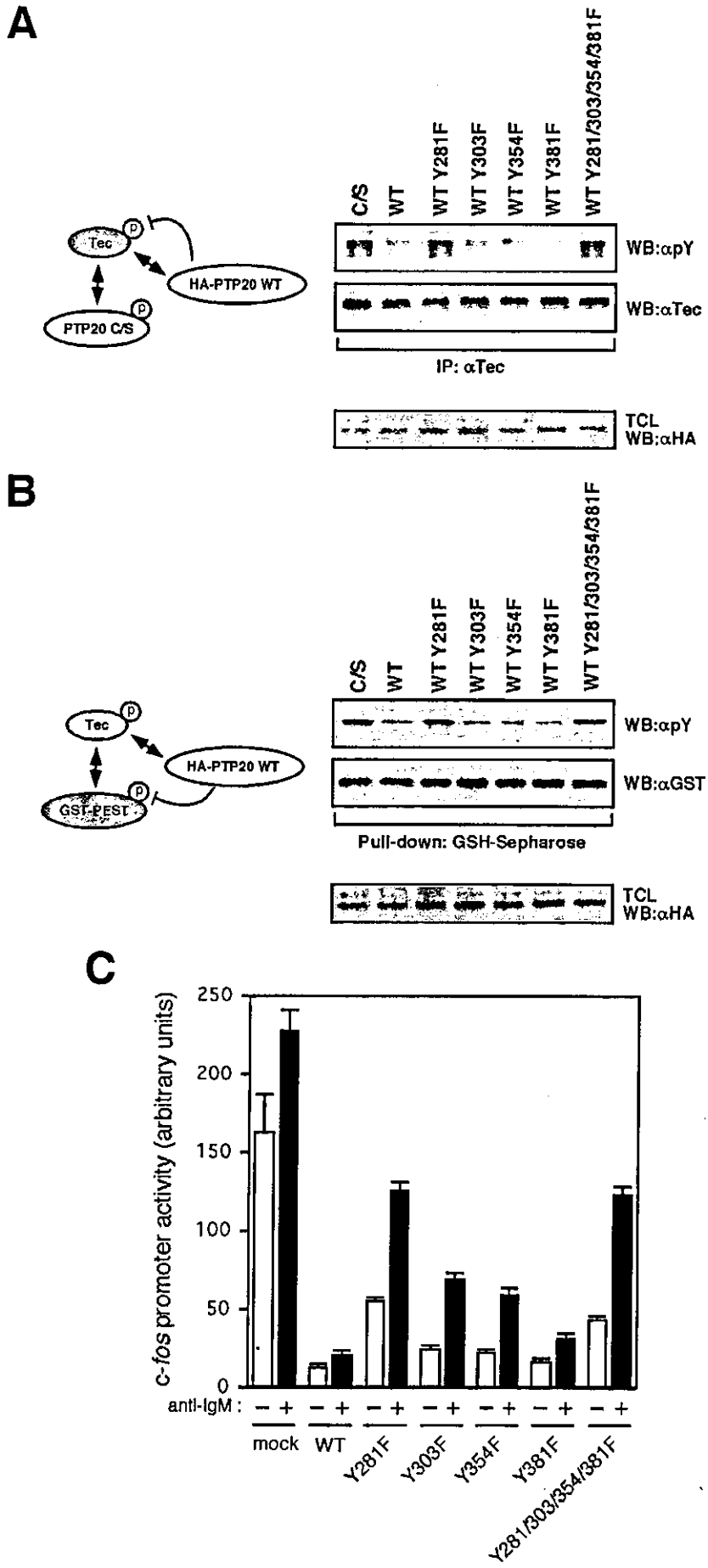

FIG. 9. **Tyrosine 281 is critical for *in vivo* phosphatase activity of PTP20.** *A*, COS7 cells were co-transfected with Tec, PTP20 C/S, and HA-PTP20 WT or its YF mutants. HA-PTP20 C/S was also included as a negative control. Cells were lysed, and Tec was immunoprecipitated with anti-Tec antibody. The immunoprecipitates (*IP*) were separated by SDS-PAGE followed by immunoblotting (*WB*) with indicated antibodies. Expression of HA-PTP20 was confirmed using aliquots of total cell lysates (*TCL*) with anti-HA antibody. *αpY*, anti-phosphotyrosine antibody. *B*, COS7 cells were transfected as above, but PEST-encoding GST-PTP20 PEST domain (GST-PEST) in place of PTP20 C/S was included. Cell lysates were subjected to precipitation with GSH-Sepharose beads and immunoblotted with the indicated antibodies. Expression of HA-PTP20 was confirmed using aliquots of total cell lysates (*TCL*) with anti-HA antibody. *C*, Ramos cells were transfected by electroporation with 2 μg of the pfos/luc reporter plasmid together with 10 μg of pcDNA3 vector (mock) or bearing PTP20 WT or its YF mutant and processed as described in legend to Fig. 8.

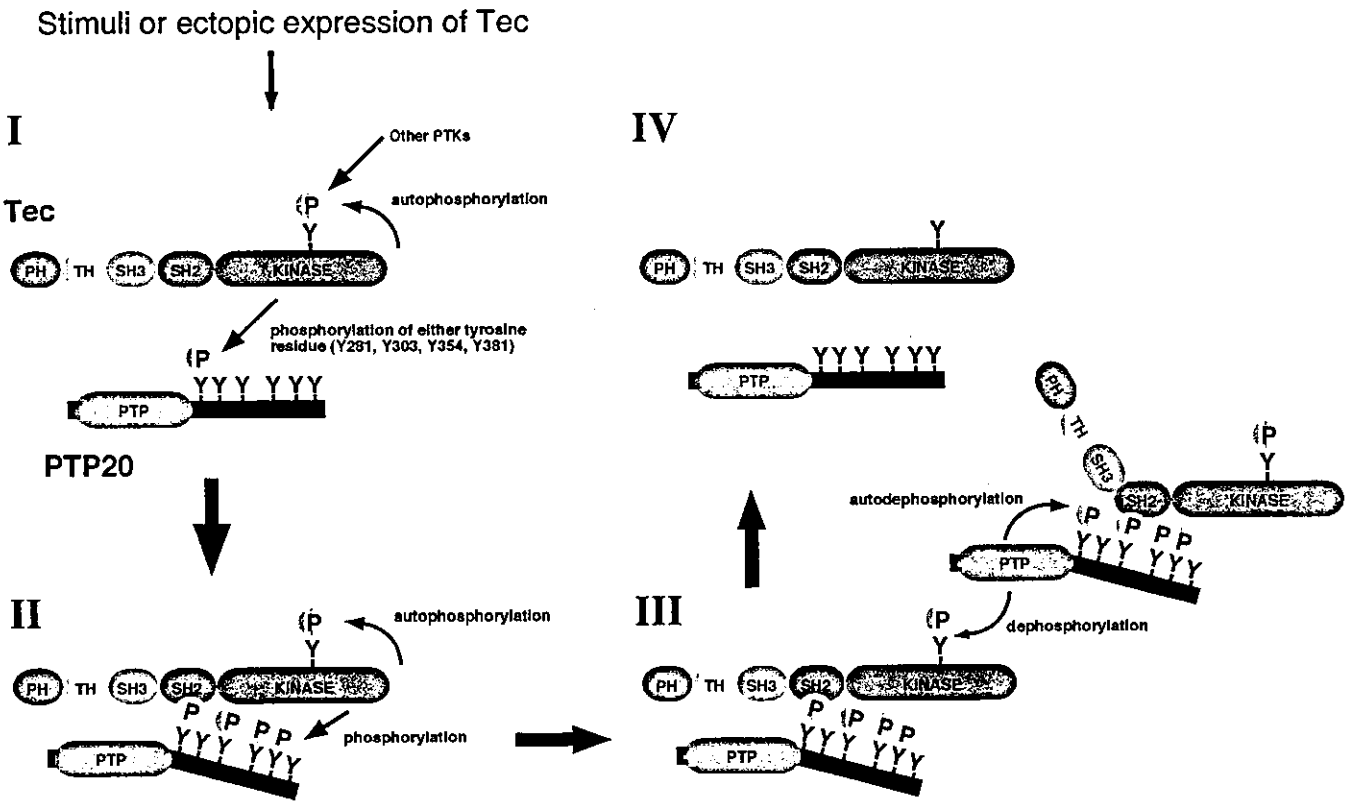

FIG. 10. **Working hypothesis for interaction of PTP20 with Tec.** *I*, upon stimuli or ectopic expression of Tec, Tec becomes tyrosine-phosphorylated and activated through autophosphorylation and other PTK catalytic activity. In turn, Tec phosphorylates tyrosine residues (Tyr-281, Tyr-303, Tyr-354, Tyr-381) on PTP20. *II*, phosphorylated PTP20 associates with Tec SH2 domain of remaining inactive Tec, thereby activating the Tec kinases. Interaction of Tec with PTP20 increases a pool of activated Tec and PTP20. *III*, activated PTP20 by phosphorylation then dephosphorylates Tec as well as PTP20 itself. Note that free of phosphorylated tyrosine 281 from association with Tec SH2 domain might be necessary for expression of PTP20 dephosphorylation activity. *IV*, finally, both Tec and PTP20 return to basal and inactive states.

dues on PTP20 caused no changes in catalytic activity by *in vitro* phosphatase assay. We have also showed that PTP20 was tyrosine-phosphorylated by Lck and Src and was associated with the PTKs (Fig. 2). However, neither the SH2 nor the SH3 domain of Lck was shown to be involved in the association with PTP20 (data not shown). Recently, another cytosolic protein-tyrosine kinase c-Abl also was shown to phosphorylate PTP20 and in turn to be dephosphorylated by PTP20 (10). Although PTP20-Tec and PTP20-cAbl interactions seem to be analogous, association between PTP20 and c-Abl is indirect, and PSTPIP, which is also a substrate of PTP20, instead serves as an adapter by bridging PTP20 to c-Abl. In contrast, association between PTP20 and Tec kinase seems to be direct, and involvement of adaptor molecules such as PSTPIPs is unlikely because the Tec SH2 domain alone could capture tyrosine-phosphorylated PTP20 (Fig. 3*D*) and, consistently, substitution of tyrosine residues on PTP20 dramatically reduced the mutual binding (Fig. 5*B*). These imply that PTP20 might be differentially tyrosine-phosphorylated by Lck, Tec, and c-Abl kinases depending on cellular context.

The Tec kinase was initially isolated from mouse liver (40) and was subsequently shown to be expressed in many tissues, including spleen, lung, brain, and kidney (41). Four Tec-related PTKs, including Btk (42, 43), Itk (also known as Emt or Tsk) (44–46), Bmx (47), and Txk (or Rlk) (48, 49), have also been molecularly cloned. Tec and the related kinases can be activated by cytokine receptors, lymphocyte surface antigens, G protein-coupled receptors, receptor type PTKs, or integrins (13, 20, 22–26). However, little is known about how the inactivation of Tec kinase is achieved. In this study, we have showed that PTP20 is a potential negative regulator in Tec-mediated signaling pathway and that the Tec SH2 domain is essential for the negative regulation by PTP20. Itk, another member of Tec family, might also be regulated by PTP20 in T cells in a similar fashion,[2] whereas Btk and Bmx seem not to interact with PTP20 (Fig. 1). Recently, the Tec SH2 domain has been shown to bind to Dok-1, which is tyrosine-phosphorylated by Tec, causing inhibition of BCR-mediated c-*fos* promoter activation (18). Another publication has demonstrated that a docking protein, BRDG1, binds to the Tec SH2 domain and acts downstream of Tec in a positive fashion in BCR signaling (50). Thus, the Tec SH2 domain might differentially participate in BCR signaling in a positive or negative way.

PTP D1, which comprises another subfamily of cytosolic PTPs, is shown to be a potential regulator and effector for not only Bmx/Etk kinase but also Tec kinase (51). The PH but not SH2 domain of Bmx/Etk is involved in the interaction with the central portion (residues 726–848) of PTP D1, and such binding is phosphotyrosine-independent, unlike PTP20-Tec interaction. Interaction between Bmx/Etk and PTP D1 stimulates the kinase activity of Bmx/Etk, resulting in an increased phosphotyrosine content in both proteins. Although it is obvious that PTP D1 is a substrate of Bmx/Etk and Tec, PTP D1 appears not to dephosphorylate the kinases. Rather, PTP D1 is a positive regulator in Bmx/Etk- and Tec-mediated signaling pathway leading to STAT3 activation. By co-transfection experiments, we observed that PTP36, which belongs to the same PTP subfamily as PTPD1, was tyrosine-phosphorylated by Tec kinase (data not shown). Thus, Tec-mediated signaling could be negatively or positively regulated by interacting with PTPs.

In conclusion, PTP20 appears to play a negative role in the

[2] S. Yamasaki and N. Aoki, unpublished data.

Tec-mediated, in particular in BCR, signaling pathways and the tyrosine phosphorylation-dependent interaction between Tec and PTP20 might form a negative feedback loop. To our knowledge this is the first report demonstrating that tyrosine phosphorylation-dependent interaction between PTK and PTP is relevant for their mutual state in some cellular context.

REFERENCES

1. Andersen, J. N., Mortensen, O. H., Peters, G. H., Drake, P. G., Iversen, L. F., Olsen, O. H., Jansen, P. G., Andersen, H. S., Tonks, N. K., and Moller, N. P. (2001) *Mol. Cell. Biol.* **21,** 7117–7136
2. Tonks, N. K., and Neel, B. G. (2001) *Curr. Opin. Cell Biol.* **13,** 182–195
3. Aoki, N., Yamaguchi-Aoki, Y., and Ullrich, A. (1996) *J. Biol. Chem.* **271,** 29422–29426
4. Cheng, J., Daimaru, L., Fennie, C., and Lasky, L. A. (1996) *Blood* **88,** 1156–1167
5. Huang, K., Sommers, C. L. Grinberg, A. Kozak, C. A. and Love, P. E. (1996) *Oncogene* **13,** 1567–1573
6. Dosil, M., Leibman, N., and Lemischka, I. R. (1996) *Blood* **88,** 4510–4525
7. Kim, Y. W., Wang, H., Sures, I., Lammers, R., Martell, K. J., and Ullrich, A. (1996) *Oncogene* **13,** 2275–2279
8. Spencer, S., Dowbenko, D., Cheng, J., Li, W., Brush, J., Utzig, S., Simanis, V., and Lasky, L. A. (1997) *J. Cell Biol.* **138,** 845–860
9. Wu, Y., Dowbenko, D., and Lasky, L. A. (1998) *J. Biol. Chem.* **273,** 30487–30496
10. Cong, F., Spencer, S., Cote, J. F., Wu, Y., Tremblay, M. L., Lasky, L. A., and Goff, S. P. (2000) *Mol. Cell* **6,** 1413–1423
11. Wang, B., Lemay, S., Tsai, S., and Veillette, A. (2001) *Mol. Cell. Biol.* **21,** 1077–1088
12. Garton, A. J., and Tonks, N. K. (1994) *EMBO J.* **13,** 3763–3771
13. Mano, H., Yamashita, Y., Sato, K., Yazaki, Y., and Hirai, H. (1995) *Blood* **85,** 343–350
14. Shiota, M., Tanihiro, T., Nakagawa, Y., Aoki, N., Ishida, N., Miyazaki, K., Ullrich, A., and Miyazaki, H. (2003) *Mol. Endocrinol.* **17,** 534–549
15. Mano, H., Yamashita, Y., Miyazato, A., Miura, Y., and Ozawa, K. (1996) *FASEB J.* **10,** 637–642
16. Mao, J., Xie, W. Yuan, H., Simon, M. I., Mano, H., and Wu, D. (1998) *EMBO J.* **17,** 5638–5646
17. Mayer, B. J., Hirai, H., and Sakai, R. (1995) *Curr. Biol.* **5,** 296–305
18. Yoshida, K., Yamashita, Y., Miyazato, A., Ohya, K., Kitanaka, A., Ikeda, U., Shimada, K., Yamanaka, T., Ozawa, K., and Mano, H. (2000) *J. Biol. Chem.* **275,** 24945–24952
19. Chen, C., and Okayama, H. (1987) *Mol. Cell. Biol.* **7,** 2745–2752
20. Yamashita, Y., Watanabe, S. Miyazato, A. Ohya, K., Ikeda, U., Shimada, K., Komatsu, N., Hatake, K., Miura, Y., Ozawa, K., and Mano, H. (1998) *Blood* **91,** 1496–1507
21. Kitanaka, A., Mano, H., Conley, M. E., and Campana, D. (1998) *Blood* **91,** 940–948
22. Machide, M., Mano, H., and Todokoro, K. (1995) *Oncogene* **11,** 619–625
23. Matsuda, T., Takahashi-Tezuka, M., Fukada, T., Okuyama, Y., Fujitani, Y., Tsukada, S., Mano, H., Hirai, H., Witte, O. N., and Hirano, T. (1995) *Blood* **85,** 627–633
24. Miyazato, A., Yamashita, Y., Hatake, K., Miura, Y., Ozawa, K., and Mano, H. (1996) *Cell Growth Differ.* **7,** 1135–1139
25. Tang, B., Mano, H., Yi, T., and Ihle, J. N. (1994) *Mol. Cell. Biol.* **14,** 8432–8437
26. Yamashita, Y., Miyazato, A., Shimizu, R., Komatsu, N., Miura, Y., Ozawa, K., and Mano, H. (1997) *Exp. Hematol.* **25,** 211–216
27. Bennett, A. M., Tang, T. L. Sugimoto, S. Walsh, C. T., and Neel, B. G. (1994) *Proc. Natl. Acad. Sci. U. S. A.* **91,** 7335–7339
28. Feng, G. S., Hui, C. C., and Pawson, T. (1993) *Science* **259,** 1607–1611
29. Vogel, W., Lammers, R. Huang, J., and Ullrich, A. (1993) *Science* **259,** 1611–1614
30. Ali, S., Chen, Z., Lebrun, J. J., Vogel, W., Kharitonenkov, A., Kelly, P. A., and Ullrich, A. (1996) *EMBO J.* **15,** 135–142
31. Boulton, T. G., Stahl, N., and Yancopoulos, G. D. (1994) *J. Biol. Chem.* **269,** 11648–11655
32. Gadina, M., Stancato, L. M., Bacon, C. M., Larner, A. C., and O'Shea, J. J. (1998) *J. Immunol.* **160,** 4657–4661
33. Tauchi, T., Feng, R., Shen, M., Hoatlin, Bagby, G. C., Jr., Kabat, D., Lu, L., and Broxmeyer, H. E. (1995) *J. Biol. Chem.* **270,** 5631–5635
34. Tauchi, T., Damen, J. E., Toyama, K., Feng, G. S., Broxmeyer, H. E., and Krystal, G. (1996) *Blood* **87,** 4495–4501
35. Welham, M. J., Dechert, U., Leslie, K. B., Jirik, F., and Schrader, J. W. (1994) *J. Biol. Chem.* **269,** 23764–23768
36. Stein-Gerlach, M., Kharitonenkov, A., Vogel, W., Ali, S., and Ullrich, A. (1995) *J. Biol. Chem.* **270,** 24635–24637
37. Stein-Gerlach, M., Wallasch, C., and Ullrich, A. (1998) *Int. J. Biochem. Cell Biol.* **30,** 559–566
38. Liu, F., and Chernoff, J. (1997) *Biochem. J.* **327,** 139–145
39. Tao, J., Malbon, C. C., and Wang, H. Y. (2001) *J. Biol. Chem.* **276,** 29520–29525
40. Mano, H., Ishikawa, F., Nishida, J., Hirai, H., and Takaku, F.(1990) *Oncogene* **5,** 1781–1786
41. Mano, H., Mano, K., Tang, B. Koehler, M., Yi, T., Gilbert, D. J., Jenkins, N. A., Copeland, N. G., and Ihle, J. N. (1993) *Oncogene* **8,** 417–424
42. Tsukada, S., Saffran, D. C., Rawlings, D. J., Parolini, O., Allen, R. C., Klisak, I., Sparkes, R. S., Kubagawa, H., Mohandas, T., Quan, S., Belmont, J. W., Cooper, M. D., Conley, M. E., and Witte, O. N. (1993) *Cell* **72,** 279–290
43. Vetrie, D., Vorechovsky, I., Sideras, P., Holland, J., Davies, A., Flinter, F., Hammarstrom, L., Kinnon, C., Levinsky, R., Bobtoe, M., Smith, C. I. E., and Bently, D. R. (1993) *Nature* **361,** 226–233
44. Heyeck, S. D., and Berg, L. J. (1993) *Proc. Natl. Acad. Sci. U. S. A.* **90,** 669–673
45. Siliciano, J. D., Morrow, T. A., and Desiderio, S. V. (1992) *Proc. Natl. Acad. Sci. U. S. A.* **89,** 11194–11198
46. Yamada, N., Kawakami, Y., Kimura, H., Fukamachi, H., Baier, G., Altman, A., Kato, T., Inagaki, Y., and Kawakami, T. (1993) *Biochem. Biophys. Res. Commun.* **192,** 231–240
47. Tamagnone, L., Lahtinen, I. Mustonen, T. Virtaneva, K., Francis, F. Muscatelli, F. Alitalo, R., Smith, C. I., Larsson, C., and Alitalo, K. (1994) *Oncogene* **9,** 3683–3688
48. Haire, R. N., and Litman, G. W. (1995) *Mamm. Genome* **6,** 476–480
49. Hu, Q., Davidson, D., Schwartzberg, P. L., Macchiarini, F., Lenardo, M. J., Bluestone, J. A., and Matis, L. A. (1995) *J. Biol. Chem.* **270,** 1928–1934
50. Ohya, K., Kajigaya, S., Kitanaka, A., Yoshida, K., Miyazato, A., Yamashita, Y., Yamanaka, T., Ikeda, U., Shimada, K., Ozawa, K., and Mano, H. (1999) *Proc. Natl. Acad. Sci. U. S. A.* **96,** 11976–11981
51. Jui, H. Y., Tseng, R. J., Wen, X., Fang, H. I., Huang, L. M., Chen, K. Y., Kung, H. J., Ann, D. K., and Shih, H. M. (2000) *J. Biol. Chem.* **275,** 41124–41132

Progress in Hematology

International Journal of
HEMATOLOGY

Stratification of Acute Myeloid Leukemia Based on Gene Expression Profiles

Hiroyuki Mano

Division of Functional Genomics, Jichi Medical School, Tochigi, Japan

Received July 28, 2004; accepted August 10, 2004

Abstract

Acute myeloid leukemia (AML) is characterized by clonal growth of immature leukemic blasts and develops either de novo or secondarily to anticancer treatment or to other hematologic disorders. Given that the current classification of AML, which is based on blast karyotype and morphology, is not sufficiently robust to predict the prognosis of each affected individual, new stratification schemes that are of better prognostic value are needed. Global profiling of gene expression in AML blasts has the potential both to identify a small number of genes whose expression is associated with clinical outcome and to provide insight into the molecular pathogenesis of this condition. Emerging genomics tools, especially DNA microarray analysis, have been applied in attempts to isolate new molecular markers for the differential diagnosis of AML and to identify genes that contribute to leukemogenesis. Progress in bioinformatics has also yielded means with which to classify patients according to clinical parameters such as long-term prognosis. The application of such analysis to large sets of gene expression data has begun to provide the basis for a new AML classification that is more powerful with regard to prediction of prognosis.
Int J Hematol. 2004;80:389-394. doi: 10.1532/IJH97.04111

Key words: DNA microarray; CD133; CD34; Transcriptome

1. Introduction

The human genome project was launched in 1991 as a joint program by the United States, the United Kingdom, Japan, France, Germany, and China. Ten years later, the first draft sequence of the entire human genome, including the nucleotide sequence of approximately 90% of euchromatin with 99.9% accuracy, was completed by the international team [1]. The total number of protein-coding genes was estimated to be approximately 31,000, only twice that for a nematode [2]. Completion of the human sequencing project was announced in 2003, with the determined nucleotide sequence encompassing >99% of euchromatin with an accuracy of 99.99% (http://www.ncbi.nlm.nih.gov/genome/guide/human). Annotation of the final sequence is still in progress but is expected to be completed soon. The postgenome era is therefore about to begin.

Compilation of the catalog of human genes has spurred the development of new technologies to investigate and characterize changes—at the gene, messenger RNA (mRNA), or protein level—in the entire gene set simultaneously. Among such genomics approaches, DNA microarray analysis has probably been the most successful to date. A DNA microarray resembles a microscope slide and contains tens of thousands of genomic fragments, complementary DNAs (cDNAs), or oligonucleotides present in individual spots. Hybridization of such arrays with labeled cDNAs derived from a sample mRNA population allows measurement of the amounts of the original mRNAs for all genes represented on the array [3]. The high density of DNA fragments achievable on currently available microarrays makes it possible to quantitate the mRNA levels for all human genes with 1 array experiment. Such profiling of gene expression in a given cell or tissue type promises to provide a new dimension to our understanding of biology.

Microarray analysis has been applied, for instance, to characterize the differentiation [4] and the inflammatory response [5] of human cells. Gene expression profiling has also helped to develop new classification systems for human diseases that had previously been categorized on the basis of pathology or cell morphology. Microarray analysis of human specimens of prostate cancer, for example, has resulted in the identification of new biomarkers that predict poor prognosis [6]. Characteristic patterns of gene expression, or "molecular signatures," are similarly expected to provide a basis for the subdivision of patients with the same clinical diagnosis into groups with distinct prognoses [7].

Acute myeloid leukemia (AML) is characterized by the clonal growth of immature leukemic blasts in bone marrow

Correspondence and reprint requests: Hiroyuki Mano, MD, PhD, Division of Functional Genomics, Jichi Medical School, 3311-1 Yakushiji, Kawachigun, Tochigi 329-0498, Japan; 81-285-58-7449; fax: 81-285-44-7322 (e-mail: hmano@jichi.ac.jp).

(BM) and can develop de novo or from either myelodysplastic syndrome (MDS) or anticancer treatment [8]. One of the most robust predictors of AML prognosis is blast karyotype [9,10]. A good prognosis is thus predicted from the presence in leukemic clones of t(8;21), t(15;17), or inv(16) chromosomal rearrangements, whereas –7/7q–, 11q23, or more complex abnormalities are indicative of a poor outcome. Such stratification is not informative, however, for predicting the prognoses of patients with a normal karyotype, who constitute approximately 50% of the AML population.

A clinical record of a preceding MDS phase is also an indicator of poor prognosis for individuals with AML. Therapy-related acute leukemia (TRL) can develop after the administration of alkylating agents, topoisomerase inhibitors, or radiotherapy. The clinical outcome of TRL is generally worse than that of de novo AML [11], and a subset of individuals with TRL also exhibits multilineage dysplasia of blood cells. Prediction of the outcome of and optimization of the treatment for each AML patient would thus be facilitated by the ability to differentiate de novo AML from MDS-related AML and TRL. However, dysplastic changes (in particular, dyserythropoiesis) in differentiated blood cells are also found not infrequently in the BM of healthy elderly individuals [12]. The differential diagnosis among AML-related disorders is therefore not always an easy task in the clinical setting, especially if a prior record of hematopoietic parameters is not available.

The application of DNA microarray analysis to AML has the potential (1) to identify molecular markers for the differential diagnosis of AML-related disorders, (2) to provide a basis for the subclassification of such disorders, and (3) to yield insight into the molecular pathogenesis of AML. In this article, I review progress related to the first 2 of these goals.

2. Identification of Molecular Markers for the Differential Diagnosis of AML

2.1. Karyotype

Given that the current classification of AML relies on blast karyotype, it would be informative to determine whether karyotype is related to the gene expression profile of blasts. In other words, is DNA microarray analysis able to substitute for conventional karyotyping?

Schoch et al performed microarray analysis with BM mononuclear cells (MNCs) isolated from individuals with AML and compared the data among the patients with t(8;21), t(15:17), or inv(16) chromosomal anomalies [13]. Each of these 3 AML subgroups was found to possess a distinct molecular signature, and it was possible to predict the karyotype correctly on the basis of the expression level of specific genes. The leukemic blasts of these subgroups of AML manifest distinct differentiation abilities, however. Blasts with t(8;21) remain as immature myeloblasts, those with t(15;17) differentiate into promyelocytes, and those with inv(16) differentiate into cells of the monocytic lineage. The overall gene expression profiles of these 3 types of blasts therefore might be substantially affected by the mRNA repertoires of the differentiated cells present within BM. It remains to be determined whether such "karyotype-specific" molecular signatures are indeed dependent on karyotype or are related to French-American-British (FAB) subtype (differentiation ability).

The gene expression profiles of BM MNCs derived from a large number of pediatric AML patients were examined by Yagi et al [14]. Clustering of these patients according to the expression pattern of the entire gene set resulted in their separation into FAB subtype–matched groups, indicative of a prominent influence of differentiated cells within BM on the gene expression profile. It may nevertheless prove possible to capture bona fide karyotype-dependent genes from large data sets with the use of sophisticated bioinformatics approaches and then to use the expression profiles of these genes for "pseudokaryotyping."

Virtaneva et al purified $CD34^+$ progenitor cells from the BM of individuals with AML and compared the gene expression profiles of the patients with a normal karyotype and those with trisomy 8 [15]. They also compared such AML blasts with $CD34^+$ fractions isolated from the BM of healthy volunteers. The use of $CD34^+$ (immature) cells for microarray analysis would be expected to reduce the influence of differentiated cells within BM on the overall pattern of gene expression. These researchers found that the AML blasts differed markedly from normal $CD34^+$ cells in terms of the gene expression profile. However, the blasts with trisomy 8 did not appear to differ substantially from those with a normal karyotype. It is possible that blasts with a normal karyotype or those with trisomy 8 are too diverse to allow identification of distinguishing gene markers.

2.2. De Novo AML versus MDS-Related AML

Although dysplasia is the diagnostic hallmark of MDS, such abnormal cell morphology is also associated with other conditions, and the subjective assessment of the extent of dysplasia suffers from the risk of variability from physician to physician. It is therefore desirable to identify molecular markers that are able to distinguish de novo AML from MDS-associated AML. It is also important to clarify whether de novo AML and MDS-associated AML are indeed distinct clinical entities or whether they overlap to some degree.

Although DNA microarray analysis is a promising tool for the identification of such molecular markers able to differentiate de novo AML from MDS-related AML, a simple comparison of BM MNCs for these 2 conditions is likely to be problematic. The cellular composition of BM MNCs differs markedly among individuals. Differences in the gene expression profile between BM MNCs from a given pair of individuals may thus reflect these differences in cell composition [16]. The elimination of such pseudopositive and pseudonegative data necessitates the purification of background-matched cell fractions from the clinical specimens before microarray analysis.

Given that de novo AML and MDS both result from the transformation of hematopoietic stem cell (HSC) clones, HSCs would be expected to be an appropriate target for purification and gene expression analysis. With the use of an affinity purification procedure based on the HSC-specific surface protein CD133, also known as AC133 [17], we have purified $CD133^+$ HSC-like fractions from individuals with

various hematopoietic disorders, and we have stored these fractions in a cell depository referred to as the *Blast Bank*. With such background-matched purified samples, we attempted to identify differences in gene expression profiles between de novo AML and MDS-associated AML [18]. To minimize further the influence of differentiation commitment of blasts toward certain lineages, we used only Blast Bank samples with the same phenotype, the M2 subtype according to the FAB classification. We thus characterized the expression profiles of >12,000 genes in $CD133^+$ Blast Bank samples from 10 patients with de novo AML of the M2 subtype as well as from 10 individuals with MDS-related AML of the same FAB subtype.

Selection with a Student t test ($P < .01$) and an effect size of ≥ 5 units for discrimination between the 2 clinical conditions led to the identification of 57 "diagnosis-associated genes," the expression profiles of which are shown in a "gene tree" format in Figure 1A. In this format, genes with similar expression patterns across the samples are clustered near each other. Patients were also clustered in this tree (2-way clustering) on the basis of the similarity of the expression pattern of the 57 genes (dendrogram at the top). All subjects were clustered into 2 major groups, 1 composed mostly of de novo AML patients and the other containing predominantly patients with MDS-associated AML. Each of these 2 main branches contained misclassified samples, however, indicating that simple clustering was not sufficiently powerful to differentiate the 2 clinical conditions completely. Furthermore, this analysis might not adequately address whether de novo AML and MDS-associated AML should be treated as distinct entities, at least from the point of view of the gene expression profile.

Decomposition of the multidimensionality of gene expression profiles by the application of principal components analysis [19] or correspondence analysis [20], for example, is often informative for such purposes. Application of the latter method to the data set of the 57 genes reduced the number of dimensions from 57 to 3. On the basis of the calculated 3-dimensional (3D) coordinates for each sample, the specimens were then projected into a virtual 3D space (Figure 1B). Most of the de novo AML samples were positioned in a region of this space that was distinct from that occupied by the MDS-associated AML specimens. However, 2 of the former samples were localized within the MDS region. These results suggest that de novo AML and MDS-associated AML are distinct disorders but that the current clinical diagnostic system is not efficient enough to separate them completely.

Instead of extracting a molecular signature from the expression profile of multiple genes, an alternative approach is to attempt to identify individual gene markers specific to either de novo AML or MDS-associated AML. We used the Blast Bank array data to identify MDS-specific markers, defined as genes that are silent in blasts from all de novo AML patients but are active in those from at least some patients with MDS-related AML [16]. This approach resulted in the identification of a single gene, *DLK*, that matched these criteria. *DLK* is expressed in immature cells [21] and is implicated in the maintenance of the undifferentiated state [22]. Selective expression of *DLK* in MDS blasts may thus contribute to the pathogenesis of MDS. Increased expression

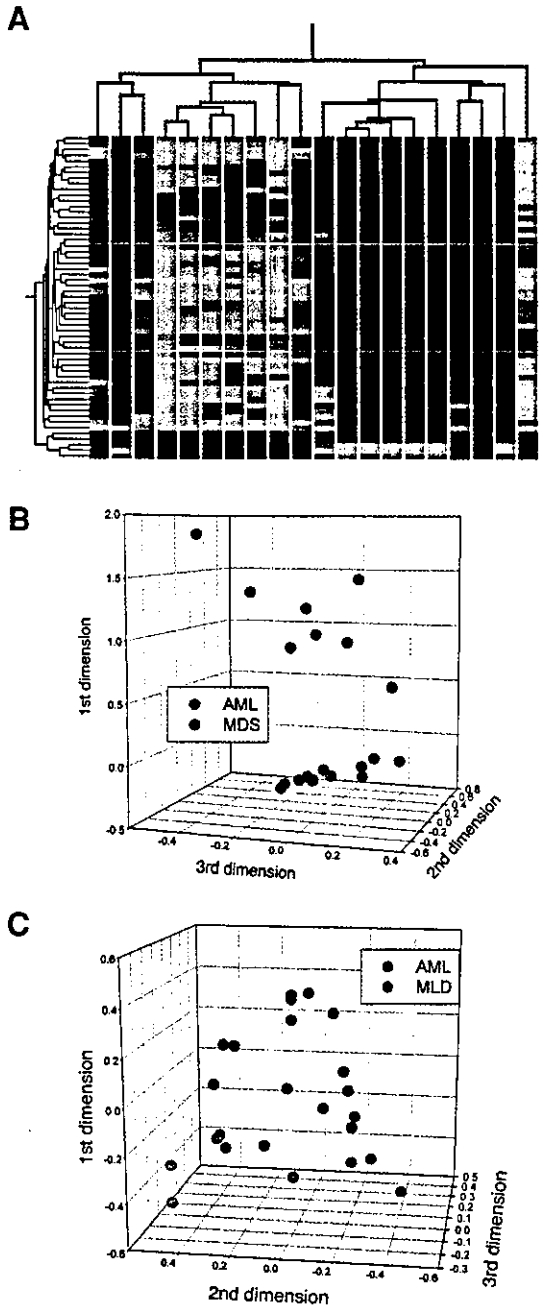

Figure 1. Correspondence analysis and 3-dimensional (3D) projection for differential diagnosis of acute myeloid leukemia (AML). A, Two-way hierarchical clustering for 57 disease-associated genes and 20 patients. Each row corresponds to a single gene and each column to $CD133^+$ cells from a patient with de novo AML (blue) or myelodysplastic syndrome (MDS)-related AML (red). The expression level of each gene is color coded, with a high level in red and a low level in green. B, Projection of the 20 specimens from (A) into a virtual space with 3 dimensions identified by correspondence analysis of the 57 genes. Patients with de novo AML (AML) were separated from those with MDS-related leukemia (MDS). C, Projection of specimens from patients with de novo AML without dysplasia (AML) or de novo AML with multilineage dysplasia (MLD) into a 3-dimensional space based on correspondence analysis of differences in gene expression. The dendrogram in (A) and 3-dimensional projections in (B) and (C) were constructed from data in [18] and [28].